

# DESIGN OF A KITE - PUMP MODEL

A Thesis Submitted  
in Partial Fulfilment of the Requirements  
for the Degree of  
**MASTER OF TECHNOLOGY**

*by*  
**K. K. TIWARI**

*to the*

**DEPARTMENT OF MECHANICAL ENGINEERING**  
**INDIAN INSTITUTE OF TECHNOLOGY KANPUR**  
**MARCH, 1983**

---

CERTIFICATE

This is to certify that the thesis entitled,  
'DESIGN OF A KITE-PUMP MODEL', by Mr.K.K.Tiwari is  
a record of work carried out under my supervision and  
has not been submitted elsewhere for a degree.

March, 1983.

  
(J.S. Goela)  
Assistant Professor  
Department of Mechanical Engineering  
Indian Institute of Technology, Kanpur  
INDIA

**CENTRAL LIBRARY**

*I. I. T., Kanpur.*

Acc. No. **A 82407**

~~A 82407~~

ME-1983-M-TIW-DES

TH  
6 21.45  
T 543d

#### ACKNOWLEDGEMENTS

I wish to express my profound gratitude to Dr.J.S.Goela, who introduced me to this field, and provided me with constant inspiration and guidance during the preparation of the thesis. I am greatly indebted to him for the invaluable encouragement and help given throughout my course of study. My association with him has been fruitful as well as memorable.

I gratefully acknowledge the interest and support of the Aeronautical Department; with special thanks to Mr.Mudappa-wind tunnel lab incharge. I am also grateful to my friend N.S. Rao for his interest and constructive suggestions; to the typist for excellent typing and Sushil for his assistance in conducting the experiments.

The list of names shall never end, because a large number of people were helpful in one way or the other. To all these Gentlemen; whose names are not included, I owe a large debt of gratitude.

-K.K.Tiwari

## CONTENTS

<u>Chapter</u>		<u>Page</u>
I.	INTRODUCTION	1
II.	SELECTION OF A KITE MODEL	7
	II.1 Flat Kite	7
	II.2 Tetrahedral and square cell kites	12
	II.3 Parafoil Kite	14
	II.4 Conyne Kite	16
	II.5 Selection of a basic Kite Design	16
III.	DESIGN AND FABRICATION OF THE KITE MODEL	19
	III.1 Kite Material and Fabrication	22
IV.	MEASUREMENT OF KITE FORCES IN THE WINDTUNNEL	26
	IV.1 Angle of attack	31
	IV.2 Data analysis	31
V.	DESIGN OF THE KITE PUMP MECHANISM	37
	V.1 Mechanism Description	38
	V.2 Working of the kite pump mechanism	40
	V.3 Determination of design Parameters	42
	V.4 Cycle performance Parameters	51
	V.5 Optimization	52
	V.6 Sensitivity Analysis	56
VI.	CONCLUSION	58
VII.	SUGGESTION FOR FUTURE WORK	59
	REFERENCES	60
	APPENDICES	

## LIST OF FIGURES AND TABLES

### Figure

- 1 Various kite models
- 2 Forces acting on a Flat Kite
- 3 The movement of center of pressure for a Flat Kite with increasing angle of attack
- 4(a,b) Rolling stabilization of a kite with dihedral
- 5(a,b) Collapse of a Parafoil kite at low angle of attack
- 6 The slot and its effect on the flow pattern
- 7 Wing tip vortices of a kite
- 8 The wind tunnel restrictions on the kite dimensions
- 9 A Conyne Kite
- 10 Experimental set up with Cathetometer
- 11 Variation of wind speed with blower voltage
- 12 Variation of kite tether tension with angle of attack "extreme points of fixation"
- 13 Variation of kite ~~tether~~ tension with angle of attack "nearest points of fixation"
- 14 The kite pump mechanism
- 15 Working of the kite pump mechanism
- 16 Several positions of the tilting bucket as it discards the water load
- 17 Variation in string tension due to tilting of the bucket
- 18 Dependence of water load on the water load parameter and dead weight parameter

**Figure**

- 19 Variation of mass flow rate with water load parameter and dead weight parameter
- 20 For a dead weight parameter of 1.122, the variation in mass flow rate and water load per cycle with the water load parameter
- 21 The dependence of water load per cycle and mass flow rate on the kite tether tension

**Tables**

- 1 Wind speed as a function of Blower Voltage
- 2 Tether tensions as a function of kites angle of attack
- 3 Bucket string tensions as it discards water by tilting

NOMENCLATURE

A	Beam cross sectional area, $m^2$
CP	Center of pressure
DW	Bucket's dead weight, Kg
g	Acceleration due to gravity, $9.81 \text{ m/sec}^2$
h	Stroke length, m
I	moment of inertia of the beam, $\text{Kg-m}^2$
K	Spring stiffness, N/cm
L	Total length of beam, m
m	mass lifted per cycle, Kg
$\dot{m}$	mass flow rate, Kg/sec
P	power, watt
PC	power coefficient
S	Kite surface area, $m^2$
T	Tether tension, N
t	time, sec
v	Linear velocity, m/sec
W	Weight, N
X	multipling factors
x	spring extension, cm
$\alpha$	angular acceleration, $\text{rad/sec}^2$
$\nu$	angular velocity, $\text{rad/sec}$
$\sigma$	density, $\text{kg/m}^3$
$\Theta$	beam angular orientation with horizontal, degrees
$\phi$	total angular rotation of the beam, degrees
$\beta$	kite's angle of attack

Subscripts

a	air
b	beam
f	final
H <sub>2</sub> O	water
L	left
R	Right
1	upward stroke
2	downward stroke

ABSTRACT

This thesis describes the design of a kite pump model for testing in the wind tunnel. The pump employs a kite to extract energy from the wind and converts it into potential energy of water. The pump operates automatically, does not need any other auxiliary energy input and is simple in design. Equations of motion of the energy system during upward and downward motions are developed to obtain performance parameters of the pump. This model pump gives a mass flow rate of 0.136 Kg/sec and power of 0.40 watts for a Conyne kite of area  $0.069 \text{ m}^2$  at the wind speed of 9 m/sec. A sensitivity analysis has also been performed to specify parameters which affect the pump performance significantly.

## CHAPTER I

### INTRODUCTION

The energy needs of mankind are increasing at a tremendous rate while the available natural resources, especially those which have served the needs of mankind until now are dwindling. It is essential, therefore, that new and yet untapped and inexhaustible sources are developed for present and future energy requirements.

One attractive source of energy is the atmospheric wind. It is estimated that approximately  $10^{14}$  KW of power could be made available from the wind. Annual kinetic energy of the wind is of the order of  $10^{17}$  KWhr and practical land based wind generators could extract as much as  $10^{14}$  KWhr of energy per year world wide [1].

The wind energy conversion systems developed so far can be classified into two main groups:

- (i) Ground based windmills
- (ii) Tether wind energy systems

Ground based windmills essentially consist of a rotor which converts wind energy into the shaft rotation. The rotor is usually mounted on a tower. The shaft rotation can be used either to pump water from a well or run a generator to produce electricity. Control mechanisms are often provided to always keep the rotor perpendicular to the wind direction.

For ground based systems cost considerations limit the height of the tower and the diameter of the rotor; therefore the rotor cannot be raised to such an altitude where steady and large wind potential is available. Further, even after a high degree of refinement in their design, the single unit power output is limited to a few MWs. Several schemes to concentrate the wind energy are being pursued to increase the output, but the economics of the machinery that intercepts the wind is still commercially uncertain.

In order to improve conversion, larger volumes of high velocity wind must be intercepted by a single machine. To achieve this, several tether based energy systems have been suggested. In these systems, a kite or a glider type system intercepts wind at those altitudes where wind potential is large and is comparatively steady in space and time.

In one type of system a windmill coupled with a generator is installed on a floating body anchored to the ground with a tether and the electrical energy produced there is transported to the ground through the conducting core of the tether. A similar scheme to use an aerodynamic platform at an altitude of 12 Km in Australia, where jet streams blow have been suggested by Fletcher and Roberts [2]. A somewhat different scheme has been proposed by Loyd [3]. He uses a glider type system tied to a tether. The design is such that as the wind blows, the glider type system rotates in a big circle whose plane is perpendicular to the wind direction. During rotation, the

system velocity is much larger than the wind velocity.

Therefore, if a windmill is mounted on the system, it will produce much larger power than that produced with a single kite situated at the same location.

Loyd has also shown that the lift produced in a high lift to drag ratio machine is sufficient to both support the kite like machine and generate power. All the above work, however, has been done theoretically and no experimental demonstration of the concept has yet been reported.

The use of Fletcher's scheme is limited as only a few locations where jet streams blow have been identified. Moreover, for the large scale power production, the weight of generators on the kite systems degrades performance and, therefore, other means of power transmission to the ground are needed.

In the second type of systems, the wind is intercepted by the floating body and its effect are transmitted to the ground through the tether. However, the useful energy conversion takes place at the ground and not on the floating body.

Goela [ 4 ] has given some basic and concrete idea about the process of power extraction by noting the fact that the tether tensions depend upon the angle of attack of the kite and that a variation in the tether tension could be used to design a kite energy conversion system as a two-stroke system with a power and a return stroke. In the power stroke the tether tension is maximized while in a return stroke it is minimized.

The changeover from power to return stroke and vice-versa takes place through a control mechanism that may be activated either remotely or by using an auxiliary string. Based on this scheme, in ref.(4) some simple energy conversion systems involving kites have been described.

In one scheme [4], the tether tension is used to rotate a wheel for half of the revolution on the ground. Just before the dead center is reached, the kite angle of attack, the projected area or both are reduced by a control mechanism. This reduces tether tension and the wheel is brought back to its original state by spending less energy. Thus a net power gain is obtained in one revolution. This is a high torque low speed system useful for low speed applications such as pumping of water. Proper synchronization of the control mechanism with the wheel rotation is very critical. It may pose practical difficulties in variable winds.

Consequently, another system called Reeling system has been described to obviate synchronization difficulty. Here, the tether tension is used to rotate a reel on the ground by unwinding it. After the kite has gone out some distance, the tether tension is reduced by a control mechanism and the rewinding of the reel is accomplished by spending less energy. Thus a net power gain is obtained. It is a high rpm low torque system therefore, the reel could be directly coupled to an electric generator through proper gearing. The disadvantage, that the power is produced in only part of the

time, can be avoided by using two kites system. This reeling system may also be used as a pump for irrigation; where only one kite is sufficient. A bucket is used to lift the water from the well. In the above design, the wind energy is first converted into rotational energy of the rotor which is then converted into the energy of the reciprocating pump. However, a direct energy conversion pump has also been suggested.

Present work can be taken as a detailed design of the above kite-pump energy conversion system. Our aim in this study is to design a Kite-pump which will be used for irrigation purposes in India. The requirements for such a system may be summarized as:

- (i) Low cost
- (ii) Simplicity of the system
- (iii) Ease of operation and maintenance
- (iv) Greater output and better conversion efficiency
- (v) Complete independence from any other energy input.

As will be shown later in this study, a kite pump can possibly satisfy the above requirements and therefore this work is directed to the design of a simple and purely mechanical Kite-pump.

This design task has been divided into four parts. First, an appropriate kite design has been selected from several kite models described in the literature [5]. The criterion for selection is described in Section II. Then we

concentrated on the design and fabrication of the kite model and this is given in Section III. After the kite model was made, it was mounted in a 3-D wind tunnel to measure tension in the kite tether. The results of this measurement are given in Section IV and its use in the design of a kite pump is given in Section V. Finally, conclusions are included in Section VI and recommendations for further work are presented in Section VII.

## CHAPTER II

### SELECTION OF A KITE MODEL

Kite flying was an amusemental and rejoiceable activity in the past, therefore, its so called selection and design were mere subjective decorations depending upon personal taste and interest that varied very rapidly like female clothing. But if the driving force changes from amusement to energy conversion the selection and design of kite should be based on the systematic considerations of its basic characteristics and requirements.

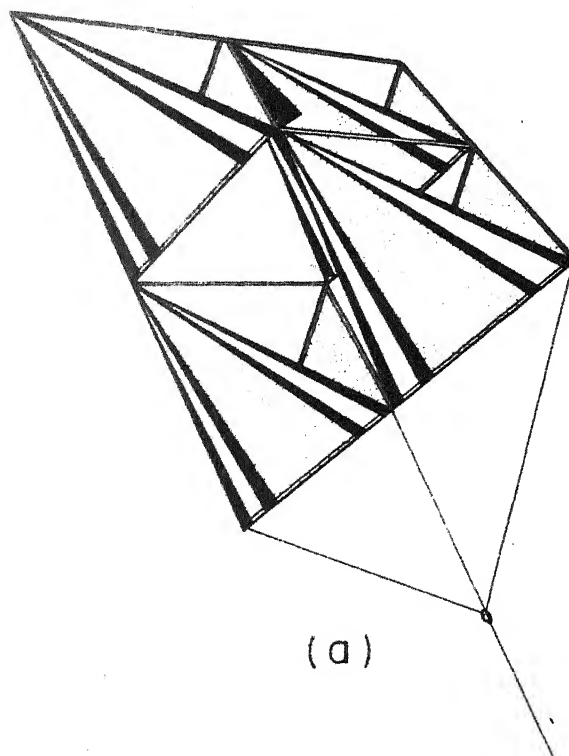
Following are the main requirements of a kite model suitable for a kite pump:

- i) stability
- ii) low cost
- iii) scaling to large sizes
- iv) high lift to drag ratio
- v) large surface area to weight ratio
- vi) should fly at low wind velocity and
- vii) should be structurally strong and durable.

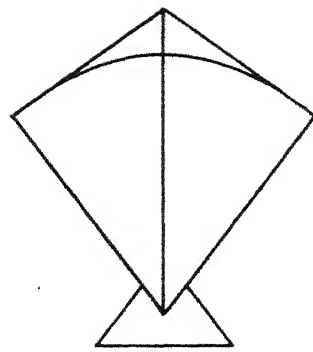
In the light of these factors four basic type of kite models (Fig.1) are examined below:

#### **II.1 FLAT KITE**

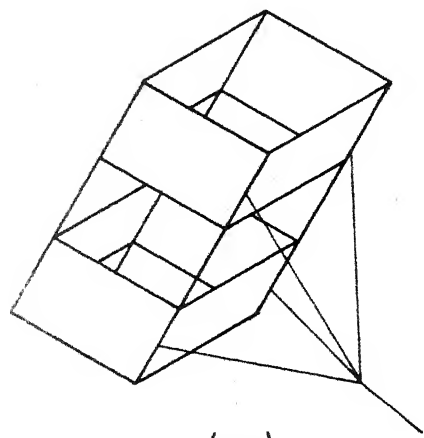
**Stability:** A flat kite is normally not as stable as we would like it to be for our requirements. This is because it is difficult to design a flat kite in which the centers of



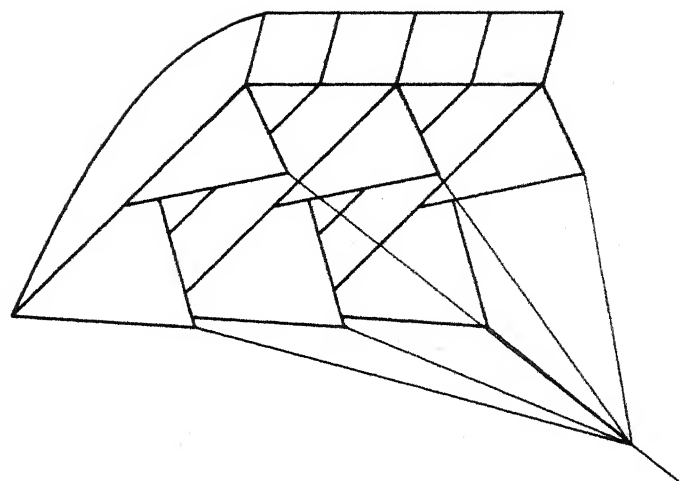
(a)



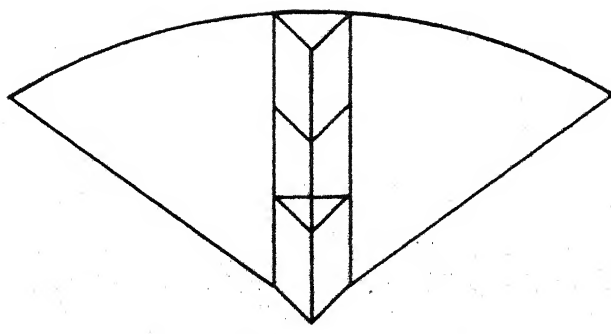
(b)



(c)



(d)



(e)

Fig. I Various kite models (a) Tetrahedral cell kite, (b) Flat kite, (c) Square cell or Box kite, (d) Jalbert para-foil, (e) Conyne kite.

pressure and gravity will coincide [6]. To see how a flat kite becomes unstable when its centers of pressure and gravity do not coincide; consider Fig.2. Fig.2(a) shows the actual flying configuration of the kite while Fig.2(b) shows the true view of the kite. The wind force can be resolved into two components; one acting along and the other perpendicular to the kite surface. The component acting along the kite surface causes the kite to spin about the center of gravity (and not about the tether axis). The perpendicular component can cause rotation about lateral or longitudinal axis of the kite. All the above modes can make the kite unstable. It should be noted, further, that the position of center of pressure and the magnitude of windforce varies with the kite angle of attack and the rolling angle.

#### Center of Pressure (CP) Movement:

In a flat plate CP moves backward as the angle of attack increases and vice versa. This is schematically shown in Fig.3. If a rising column of air strikes the leading edge, the angle of attack of the kite increases causing CP to move to the rear. This results in increased lift at the rear end. Due to this the rear end of the kite rises and causes the angle of attack to decrease. Thus, the flat kite is stable [7].

Attaching a tail to a flat kite normally improves its stability but the tail increases the kite weight without increasing the lifting surface area which is undesirable. The flat kite flies exceptionally well in light to gentle winds.

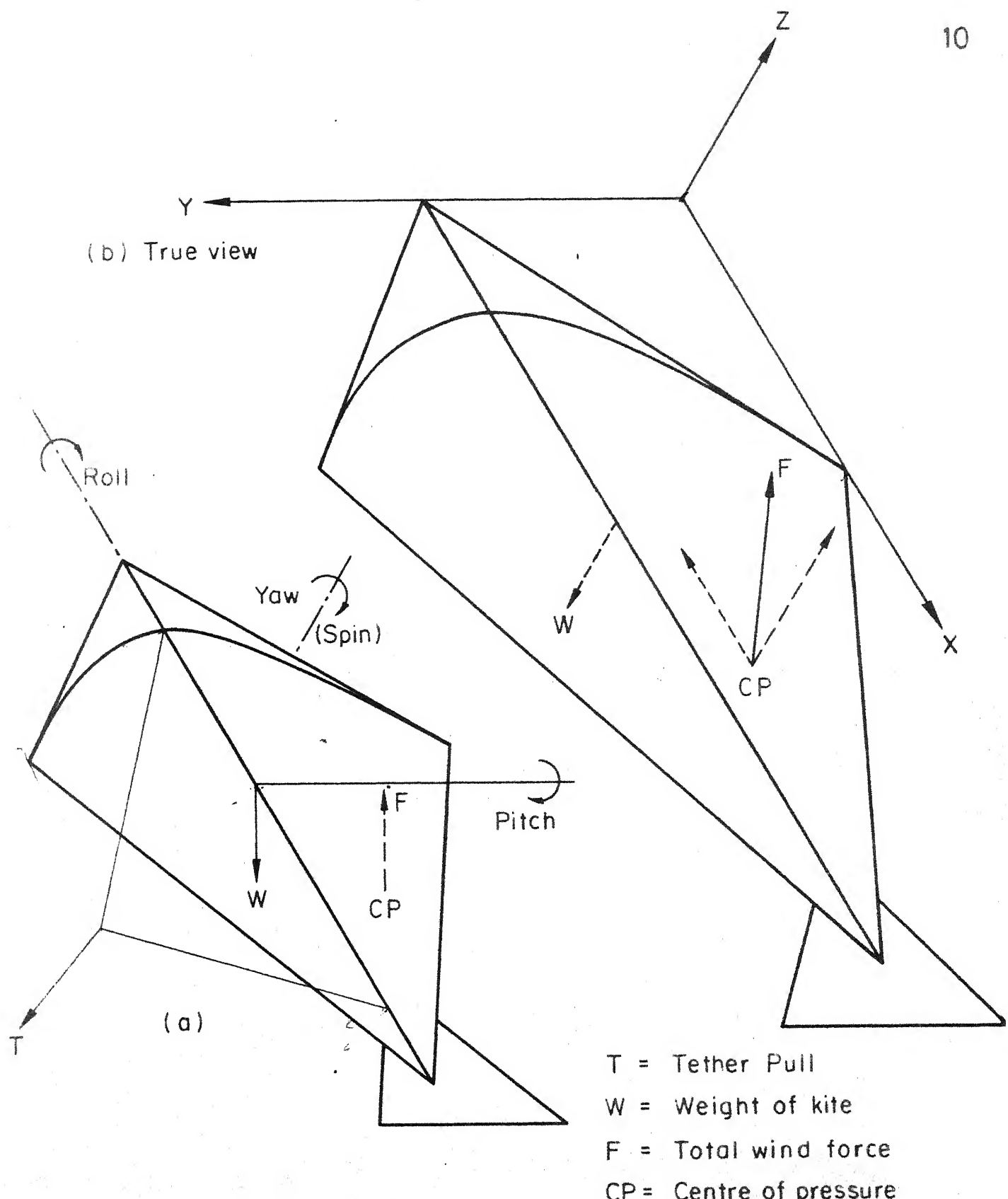


Fig. 2 Forces acting on a flat kite and its stability

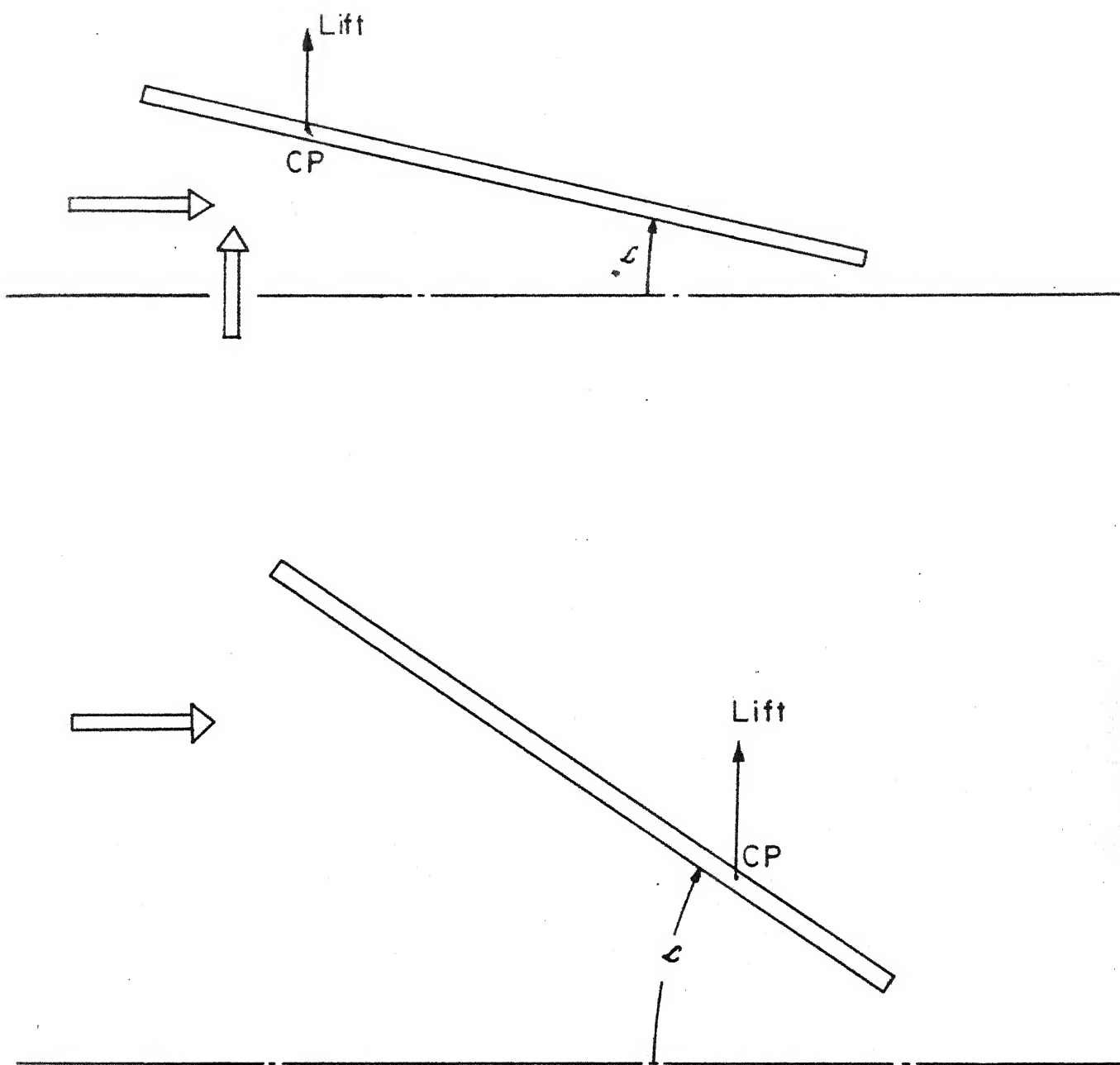


Fig. 3 The movement of centre of pressure for a flat kite with increasing angle of attack.

Scaling beyond a certain size is not desirable in a flat kite, because, of worsening structural rigidity. As compared to other models it is cheaper; but its lift to drag ratio is low because it is not an airfoil section.

There are several models like Delta kite and Malay kite where surfaces have some curvature instead of being perfectly flat. For low angle of attack, a flat kite has greater lift than the curved surface kite, which has higher drag. Therefore, for low angle of attack a flat kite is preferable to a curved surface kite. However, the trend reverses at higher angle of attack.

### III.2 TETRAHEDRAL AND SQUARE CELL KITES

These are cellular kites having excellent stability but these kites require moderate to strong winds to stay aloft. The stability is due to the structure called DIHEDRAL whose action is shown in Fig.4(a). If the kite rolls slightly to the right, the tip of the right wing moves forward and the wind force on the wing increases. At the same time, the wind force acting on the left wing reduces, because, its projected area in the direction of wind decreases. The kite is, therefore, subjected to more wind force from the right wing and less force from the left wing. This causes the kite to roll back to the left. Two arrangements of dihedrals are possible [ Fig.4 (b) ].

The scaling of cellular kites to large sizes is excellent because of their three dimensional structure. However, their L/D ratio is comparatively small. Also, they have low surface

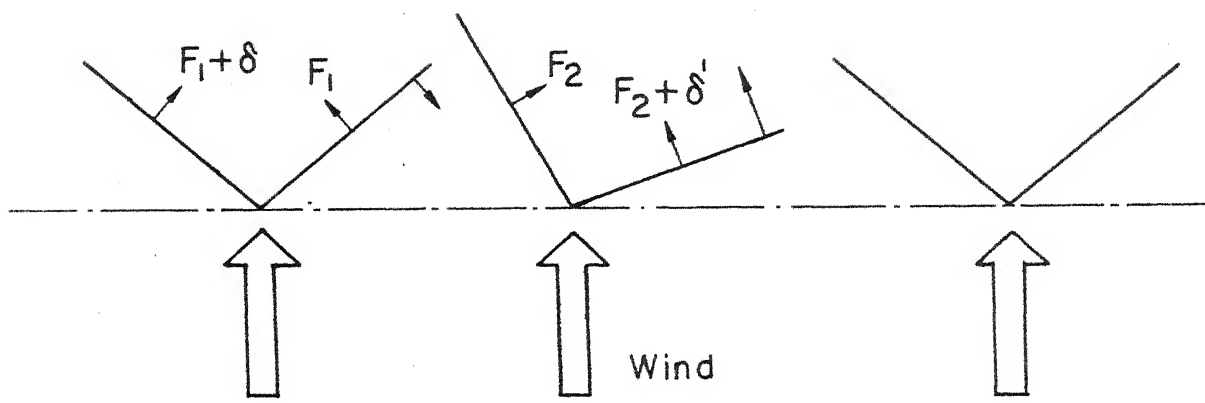


Fig. 4(a) Rolling stabilization of a kite with dihedral  
(Top view)

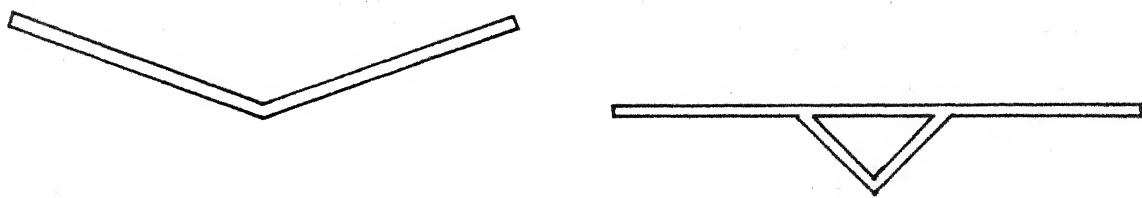


Fig. 4(b) Two possible dihedral structures.

area to weight ratio. Their cost is somewhat higher. This type of kites can be recommended for those locations where strong winds blow all year around.

### II.3 PARAFOIL KITE

This kite is a combination of an airfoil, uses inflation principles of a wind shock and some characteristics of a parachute. The net result is a highly efficient kite with great lifting power. Made entirely from fabric, this type of kite does not have any supporting structure. Scaling to large sizes is possible and the cost is not very much. Stability is due to the front flaps connecting the bridle lines and the parafoil mainbody.

Two points connected with parafoil kite should be noted. First, as its angle of attack increases, the resultant wind force increases in magnitude and CP moves towards the leading edge. This behaviour is just opposite to that of a flat kite. This increases the angle of attack further, and the cumulative effect makes the parafoil kite unstable in this sense.

Secondly, the angle of attack of the parafoil kite cannot be reduced beyond a certain limit because the kite is flexible. Otherwise, the hollow space will collapse and the kite shall stop discharging its functions properly. This is shown in Fig.5.

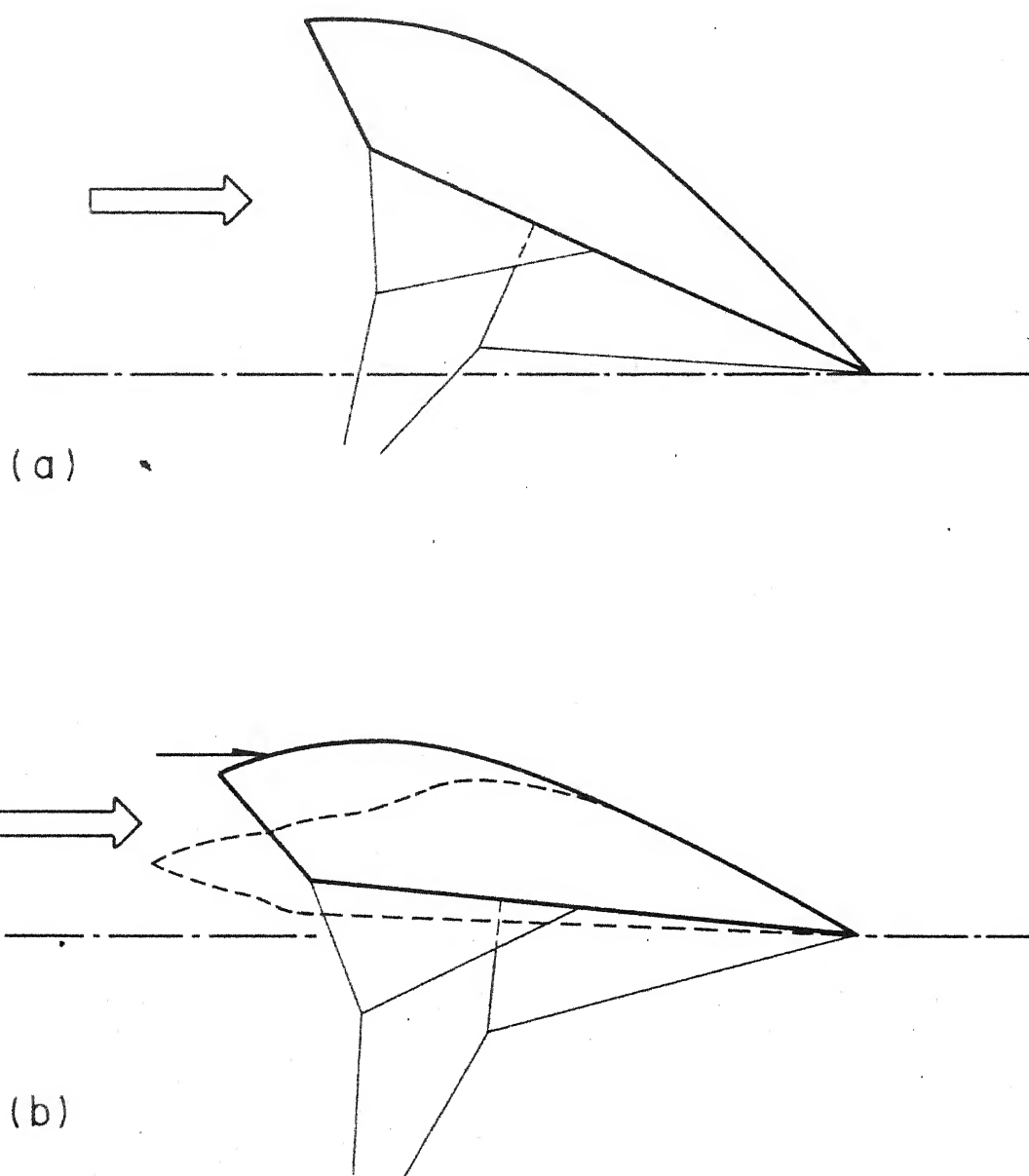


Fig.5 Collapse of a parafoil kite at low angle of attack

#### II.4 CONYNE KITE

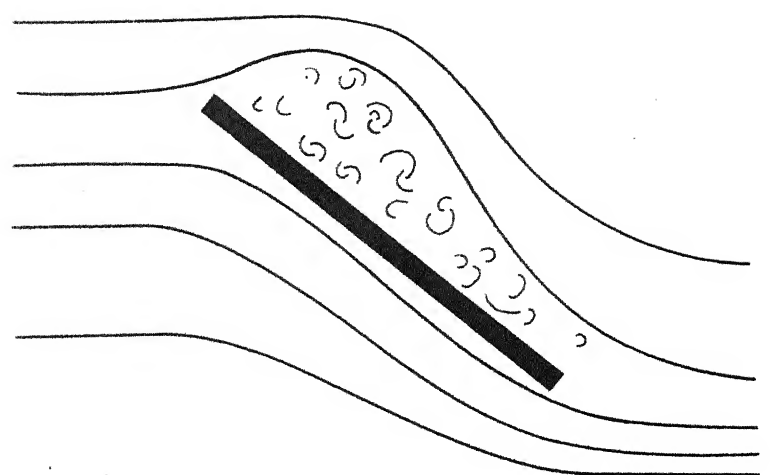
It is essentially a triangular box kite with wings. It incorporates the lifting advantage of a flat kite with the stability of a cellular kite. Actually, lift and stability cannot flourish together, one has to be sacrificed for the sake of the other. Parafoil is not designed with dihedral, therefore, it gives less stability but large lift. A Conyne Kite is very stable because it has dihedral.

SLOTS are incorporated in the structure, in order to improve the airflow conditions at higher angle of attack. Since streamlined flow gives more lift it is better to have slots in a kite structure. Further, it is beneficial to locate these slots near the leading edge. The function of a slot is shown in Fig.6. The characteristics of a Conyne Kite lie somewhere between that of a flat kite and a cellular kite. This kite has good stability, low cost, can fly in winds as low as 3 Km/hr, and could be scaled to large sizes. However, its L/D ratio is smaller than that of a parafoil.

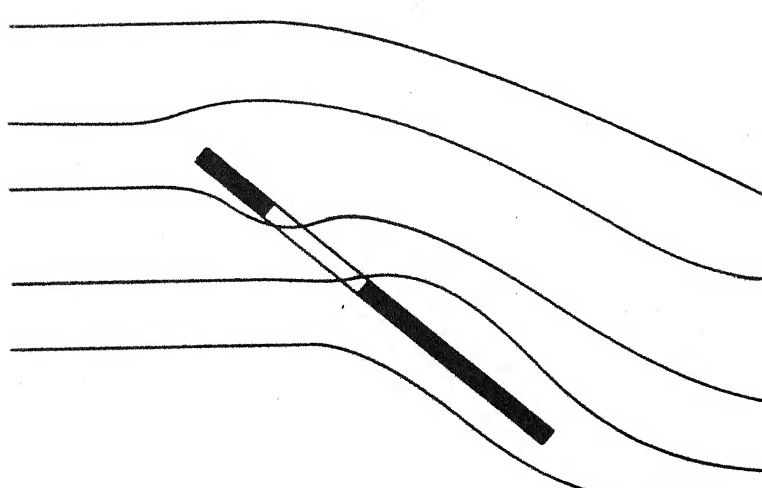
#### II.5 SELECTION OF A BASIC KITE DESIGN

The high instability inherent in a flat kite, low surface area to weight ratio of a tetrahedral kite and the possibility of a parafoil kite to collapse at low angle of attack have restricted their use in wind tunnel testing.

However, to gain the first hand experience, the flat kite and the parafoil kite models were made and tested in the



(a)



(b)

Fig.6 The slot and its effect on the flow pattern

wind tunnel. Both these models were found to be very unstable and not appropriate for our application. A Conyne Kite is stable, reasonably strong and produces reasonable value of L/D ratio. This type of kite model was also made and tested in the wind tunnel. It proved better than the other models tested. For these reasons, we decided to use it for further experimental work.

## CHAPTER III

### DESIGN AND FABRICATION OF THE KITE MODEL

For the Conyne type of the kite that we wish to design, the geometric dimensions have been taken from reference [ 5 ]. However, it is desirable to take a kite with as large span as possible to minimize the effect due to tip vortices. This is explained in Fig.7. As the air flows over and under the kite, it produces a region of low and high pressure, above and below the surface respectively. Because of the finite span, air under the wings seeks the low pressure region above the wing, by "spilling over" the tips. Eddies are formed in this manner at the tips, causing the streamlines to form vortices. The turbulence thus produced, absorbs energy and increases the drag. At the same time the lift near the tip is reduced. Wing tip vortices are unavoidable, but their effect can be reduced by increasing the aspect ratio. Unfortunately, aspect ratio is also limited due to structural reasons.

In attempting to design as large a kite as possible for obtaining more power, care must be taken to keep the ratio of kite area to wind tunnel cross sectional area, small. We have a maximum kite rotation of  $32^\circ$ , at the top and bottom dead points along with a 30 cm stroke length in 60 cm vertical space available in the wind tunnel. Subtracting 8 cm from the top and bottom to keep the kite out of boundary layer and for a kite rotation of  $32^\circ$ , the total length of the kite .

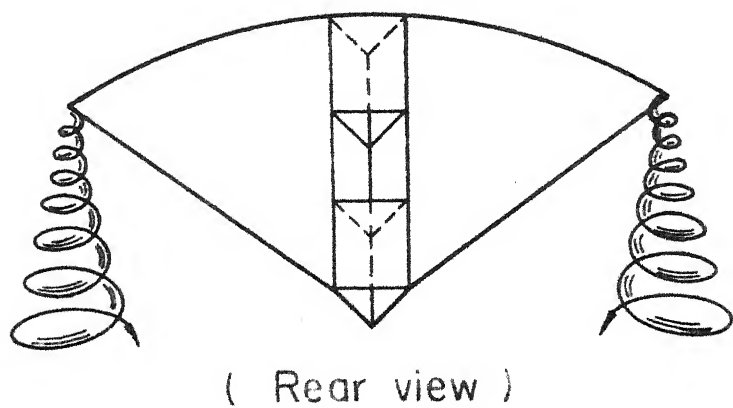


Fig.7 Wing tip vortices of a kite

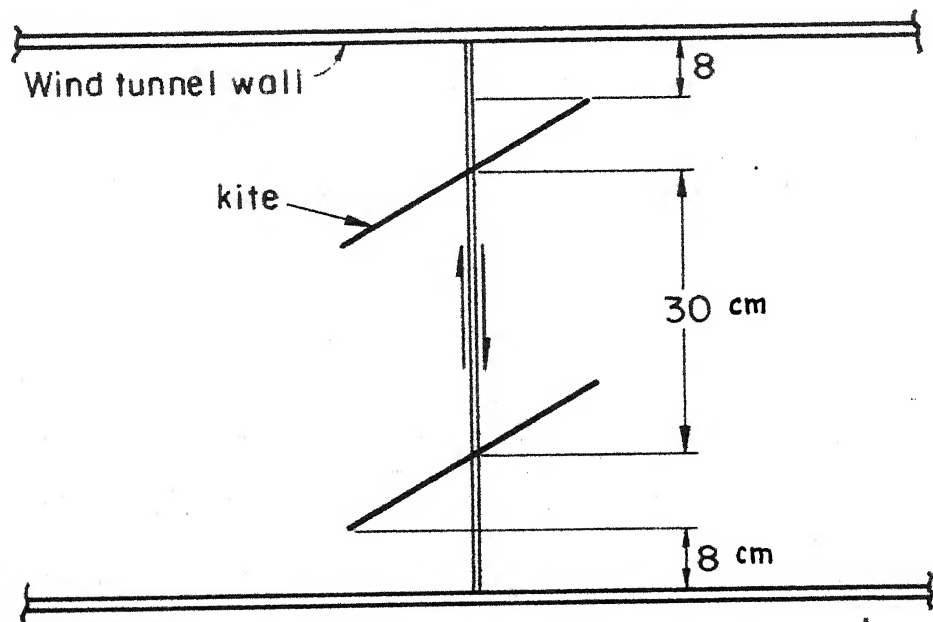


Fig.8 Wind tunnel restrictions on kite dimensions.

should be approximately 28 cm (Fig.8) (for one half of the kite length L is 14 cm as calculated from  $L \sin 32^\circ = 7.0\text{cm}$ ).

The width of the kite cannot be increased more than 60 cm, because of the presence of two steel rods which were used to facilitate vertical movement of the kite. Bigger kites block the airflow and may change the wind stream characteristics up and downstreams. Under these circumstances the proportionate dimensions were selected. The dimensions of the kite are shown in Fig.9.

### III.1 KITE MATERIAL AND FABRICATION

There are three main parts in a kite. These are: tether, sail and the frame. The tether is invariably made from either nylon or mylar. In our case, we have used nylon. For sail we used ripstop nylon especially imported from the United States.

The ripstop nylon is perhaps the lightest, and the most durable fabric. Tightly woven, this fabric has minimal porosity. Inferior quality of this fabric may be Urethane coated to give zero porosity. It is excellent to work with, capable of withstanding large pressure and easy to sew.

In India, good plastic sheets, Parachute cloth, or ordinary cotton can serve the purpose; but the dope must be applied to make it airtight. Moreover, the cloth must be tight on to the frame from all sides, otherwise strong wrinkles may appear after dope dries away. More than one layer of dope

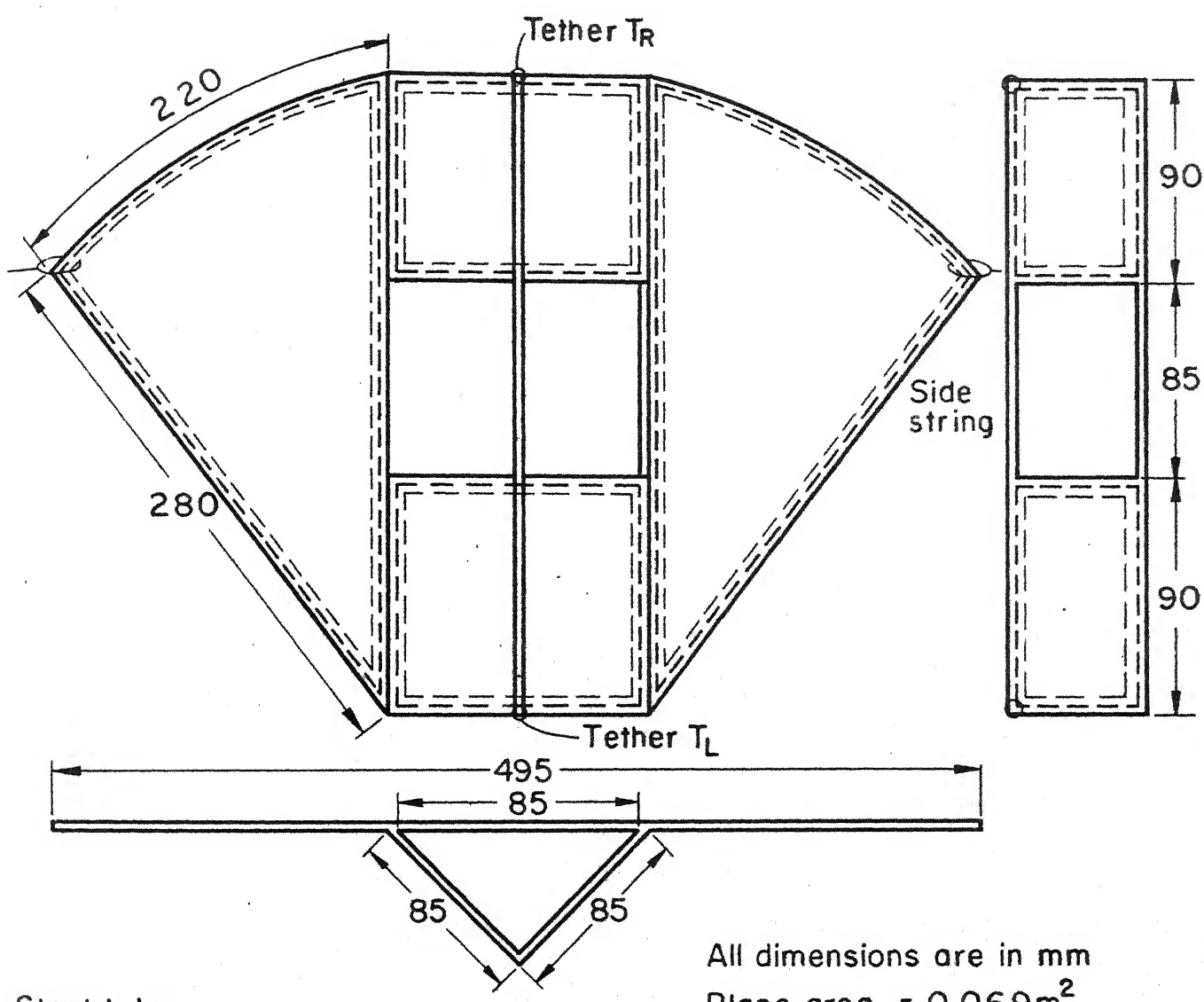


Fig. 9 The detailed Conyne model

may be applied to get good results.

The working and performance of the kite is better with fabric, rather than plastic or tissue paper. Sewing is recommended to glueing because of higher pressure forces that are to be encountered during the energy conversion. Other useful sail materials could be Tyvek and Mylar. Tyvek is a spun bonded Olefin. Stiff, slippery and drapable (i.e. confirms to the wind force more easily) paper. It can be sewn, glued or taped [ 8 ]. Mylar is a transparent polyester film having very high tensile strength. It cannot be sewn and is somewhat tricky to heat seal or glue, though contact cement works well.

For the frame material, we used, bamboo sticks and stainless steel tube (surgical tubes). The latter was found to be better for our requirement. The surgical tube is very expensive. It gives a light kite frame with high strength, stiffness and elasticity. The stainless steel tubing is difficult to weld. For smaller kites, brazing can be done. For bigger kites, metal arc inert gas welding is the best. However, tubes having carefully prepared notches on their one side can be joined with araldite. Before applying this adhesive, the joint should be carefully tied with a fine wire. This construction gives a **clearcut** and sharp featured frame. Three other very good materials which may also be used are aluminum tube, fiberglass rod and tubular graphlex.

Aluminum tubing is a good compromise between strength and price. It is less elastic and difficult to weld. For smaller models, Capillary tubes are not available. However, for bigger kites it may serve useful purpose. Fiberglass rods are heavier than aluminum, more durable and more flexible. Tubular Graphlex (Graphite-fiberglass struts) is costly, light, sturdy and collapsible. It is useful especially for larger kites. The material is a filament-wound fiberglass, with graphite reinforcements running lengthwise. It is strong, springy and light. The ferrules are short fiberglass fittings that slip snugly inside the tube. They are used to extend the tube length. The tubes can be cut with a hacksaw, sanded or filed smooth, and drilled.

## CHAPTER IV

### MEASUREMENT OF KITE FORCES IN THE WIND TUNNEL

In order to properly design a kite pump for wind tunnel testing, it is necessary to first measure tether tension as a function of kite angle of attack. A Conyne type of model was made following the procedure outlined in Section III and mounted in the tunnel as shown in Fig.10.

The wind tunnel is a low speed wind tunnel having 3-D test section 168x91.5x61 cm. The wind velocity in the tunnel was measured using a micromanometer with resolution of  $\pm 0.0025$  mm and accuracy of  $\pm 0.005$  mm of manometer fluid (Ethyl Alcohol). In the tunnel, the wind velocity can be changed by varying the supply voltage of the blower. The wind velocity as a function of the blower voltage was obtained and is plotted in Fig.11, and the details are shown in Table 1.

The kite was briddled with two tethers, one tied near the leading edge while the other tied near the trailing edge. The two tethers pass through two holes in the bottom cover of the wind tunnel. To measure the tether tensions we have used hanging weights directly connected to the tethers coming out of the lower wind tunnel covering. In the readings noted in Table 2 the pans weights are included to get the total tensions. Spring balances should not be used to measure the tether tensions, as any deflection in the system may change the models angle of attack [9].

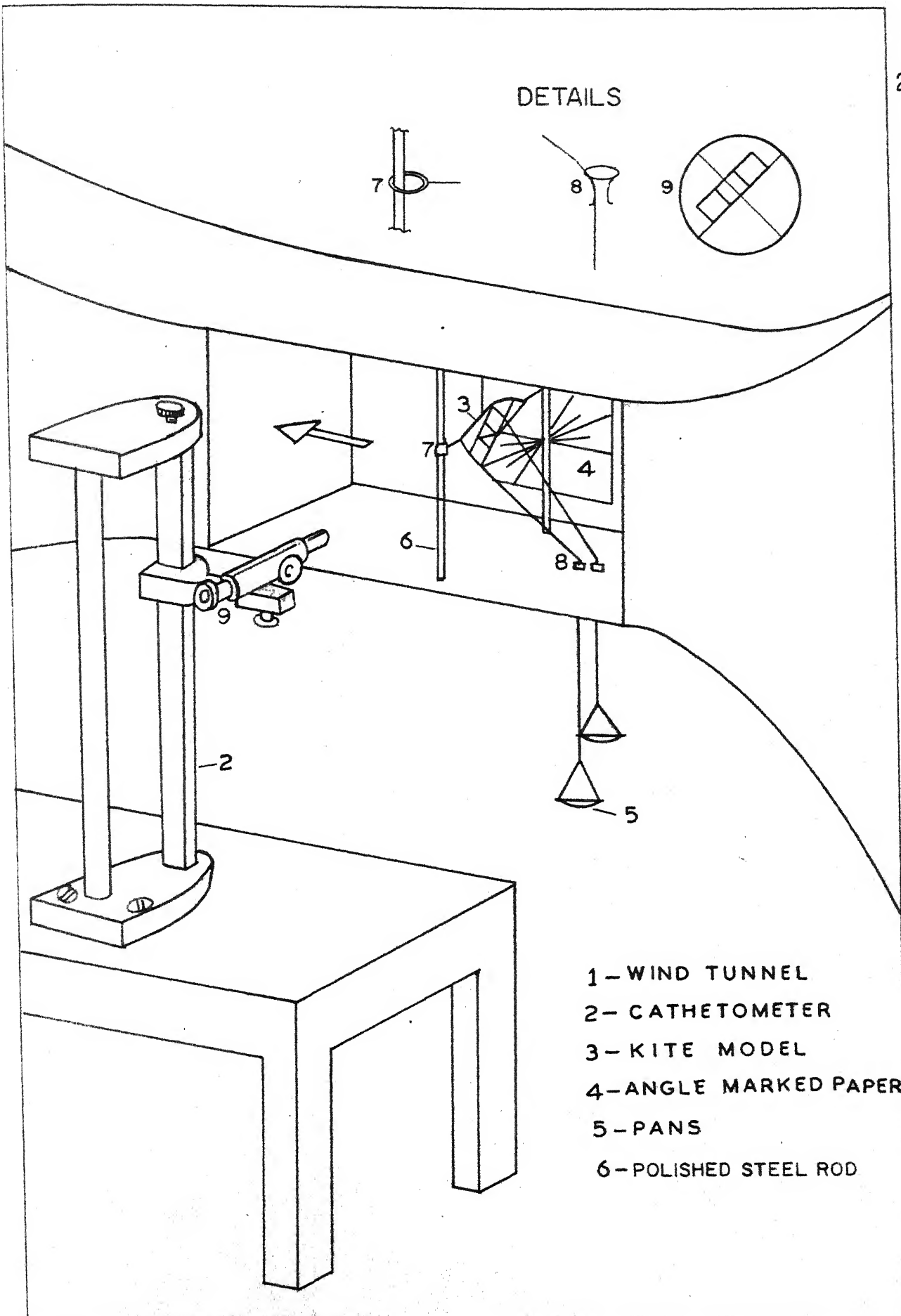


FIG.10 THE EXPERIMENTAL SET-UP FOR MEASURING KITE TETHER TENSIONS.

TABLE 1THE WIND SPEED AS A FUNCTION OF BLOWER VOLTAGE

Atmospheric pressure = 73.6 cm of Hg

Discharge section temperature = 22°C

Formula used: Velocity  $V = 59.4 (h)^{1/2}$  fps

$h = (\text{Initial manometer reading} - \text{Current manometer reading})$ , in  
 Initial Reading = 1.259 in.

S.No.	Blower Voltage, Volts	Micromano-meter Reading, in.	h, in	V fps	V m/sec
1	0	1.259	-	-	-
2	20	1.204	0.550	13.93	4.22
3	40	1.091	0.168	24.35	7.37
4	50	0.975	0.284	31.65	9.59
5	60	0.775	0.484	41.32	12.52
6	70	0.584	0.675	48.80	14.78
7	80	0.319	0.940	57.59	17.45

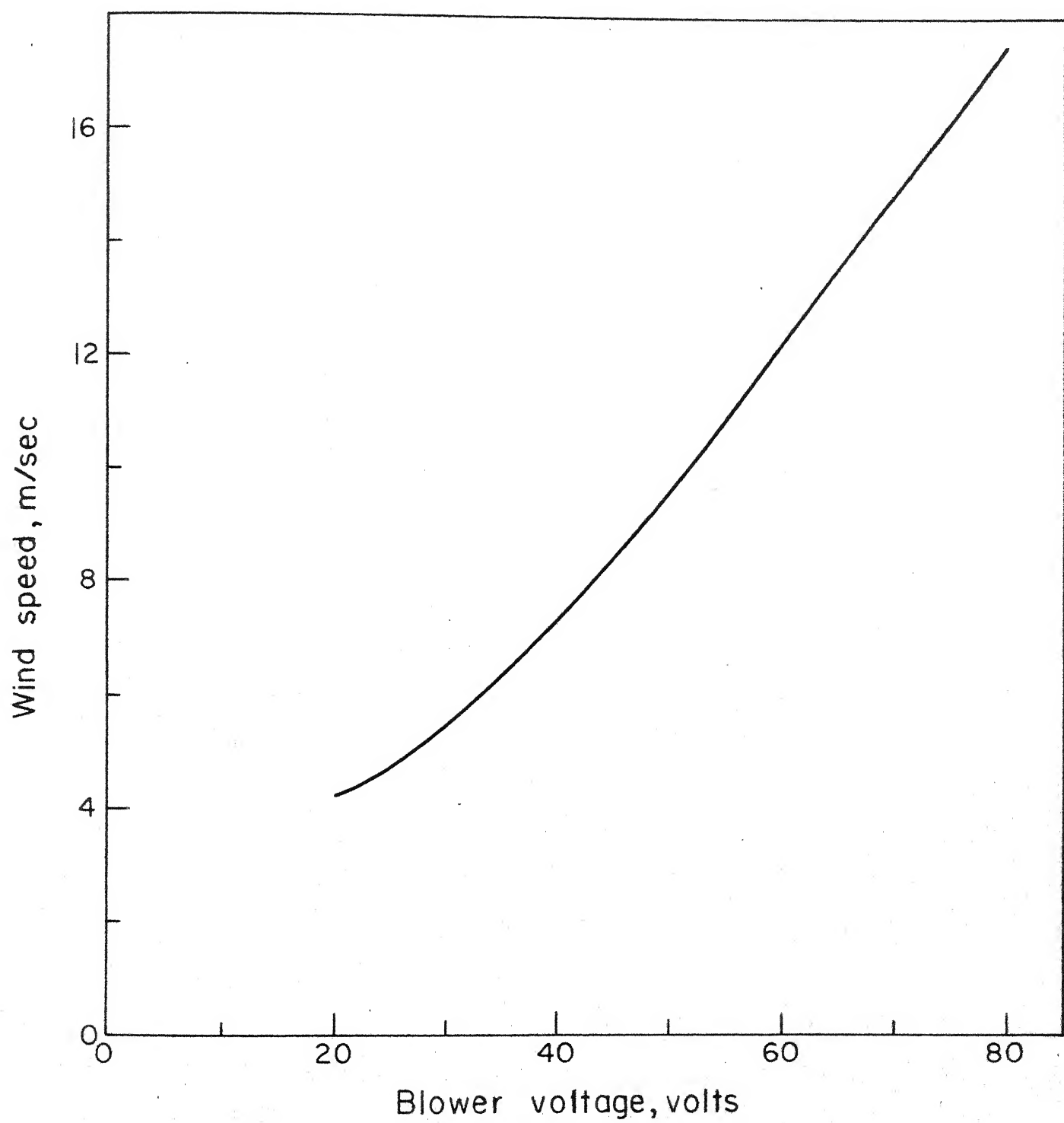


Fig. 11 Variation of wind speed with blower voltage

To obtain accurate value of tension, the tether should pass through a smooth and continuously trouble free passage. We have fixed a glass tube, blown to take the shape of a funnel, at the lower covering. However, frictionless pulleys with ball-bearings can also be used. The disappointing problem of tether going out of the pulley groove can be avoided by taking a complete turn over the pulley. To constraint the kite to move in a vertical straightline, two polished steel tubes have been used. A light, hard and polished ring passes over these rods. These rings are tied to the Kite's extreme side points with a string. Superfinishing of the tubes and rings is the key point in reducing the friction in this arrangement.

Because of drag, the kite may move downstream side. To ensure frictionless up and down kite motion, the weights must be added in the pans till the side threads come in straight line and the rings become free and loose. Previously, to ensure the kite stability, threads have been attached between the extreme side points and the top covering of wind-tunnel and it has been reported that the tension in these threads were negligible [ 4 ]. While conducting this experiment it has been observed that with this arrangement the angle of attack changes as the kite moves up vertically. Moreover the tension in the side threads may not be negligible.

One more technique to constraint the kite to move in vertical straight line has been tried. In this technique two pairs of pulleys over which a full turn thread was passing, were used. But because of structural constraints of the test section,

it did not turn out to be a rigid arrangement.

#### IV.1 ANGLE OF ATTACK

Measurement of the angle of attack is the most important, but at the same time a difficult job, because the kite + tether system is a highly flexible network and the conventional method of measuring the angle of attack (used for Aerofoil section) fails.

The Cathetometer, the familiar comparator, consisting of a telescope sliding on a vertical scale and provided with a vernier, gives the excellent solution to this problem. It leaves the kite arrangement totally undisturbed. The angles have been measured from outside the tunnel, looking through the front glass wall. A paper is pasted at the back wall, having angles marked from 0 to 360°. Since the eyepiece containing the cross wire can be easily rotated, the telescope is focussed on the kite centerline. Then the cross wire is turned so that it coincides with the kite centerline. The telescope is then focussed at the back wall "angle paper" without disturbing the cross wire. This gives the exact and actual angle of attack in any kite position. We have changed the angle of attack by varying the tether tensions.

#### IV.2 DATA ANALYSIS

Table 2 shows the recorded data of the tether tensions as function of the angle of attack of the kite at wind speed of 9 m/sec. To investigate the effect associated with a

TABLE 2TETHER TENSIONS AS A FUNCTION OF KITE'S ANGLE OF ATTACK

Blower Voltage = 46 Volts

Wind Velocity = 9 m/sec

"Extreme" Configuration"Nearest" Configuration

S.No.	$\beta$ degree	$T_L$ Newtons	$T_R$ Newtons	$T_{TOTAL}$ Newtons	$\beta$ degree	$T_L$ Newtons	$T_R$ Newtons	$T_{TOTAL}$ Newtons
1	8	0.78	5.40	6.18	10	2.35	4.90	7.25
2	12	1.37	5.68	7.05	12	2.84	4.70	7.54
3	14	1.66	6.67	8.33	15	3.72	4.41	8.13
4	20	2.35	7.25	9.60	21	5.92	4.31	10.23
5	27	2.85	7.25	10.10	23	5.19	3.72	8.91
6	30	3.52	7.40	10.92	24	5.29	3.43	8.72
7	32	3.83*	7.25	10.08	30	5.98	2.74	8.72
8	35	"	6.67	10.50	31	5.78	2.74	8.52
9	38	"	6.18	10.01	35	6.47	1.76	8.23
10	40	"	4.70	8.53	39	6.47	1.27	7.74
11	46	"	3.72	7.55	44	6.67	0.78	7.45
12	50	"	2.74	6.57	45**	6.96	0.78	7.74
13	60	"	1.76	5.59				
14	64	"	1.27	5.10				
15	68	3.83	0.78	4.61				

\* The kite does not remain in equilibrium if any attempt is made to increase the angle of attack beyond  $32^\circ$  by increasing  $T_L$ . The only way left is to reduce  $T_R$ .

\*\* Beyond the angle of attack of  $45^\circ$ , kite does not remain in equilibrium. It comes down.

variation in the attachment point of the tether to the kite, we have taken measurements in two configurations - one when the tether is fixed to the trailing edge ("extreme" configuration) and the other when the tether is tied at a point which is a small distance from the trailing edge ("nearest" configuration). In both the above configurations, the second tether is attached to the leading edge. The data for "extreme" and "nearest" cases are shown in Fig.12 and Fig.13 respectively.

It is evident from Fig.12 that as the angle of attack increases, both  $T_R$  and  $T_L$  increase. However, when the angle of attack increases beyond  $32^\circ$ ,  $T_R$  reduces and  $T_L$  becomes constant. One reason for this decrease in  $T_R$  could be due to the movement of center of pressure towards the trailing edge. The effect of movement of CP towards the trailing edge could be seen more clearly in Fig.13. Here as the angle of attack increases,  $T_R$  decreases but  $T_L$  increases.

For the kite pump the "extreme" configuration is more appropriate to the "nearest" configuration. This is due to the following reasons: The maximum tether tension is larger ( $= 11$  N) for "extreme" configuration than for "nearest" configuration ( $= 9$  N). Another important measure - the difference between the maximum tether tension and the minimum tether tension at the lower angle of attack is larger in the case of "extreme" configuration ( $= 4.82$  N) than in the case of "nearest" configuration ( $= 1.6$  N).

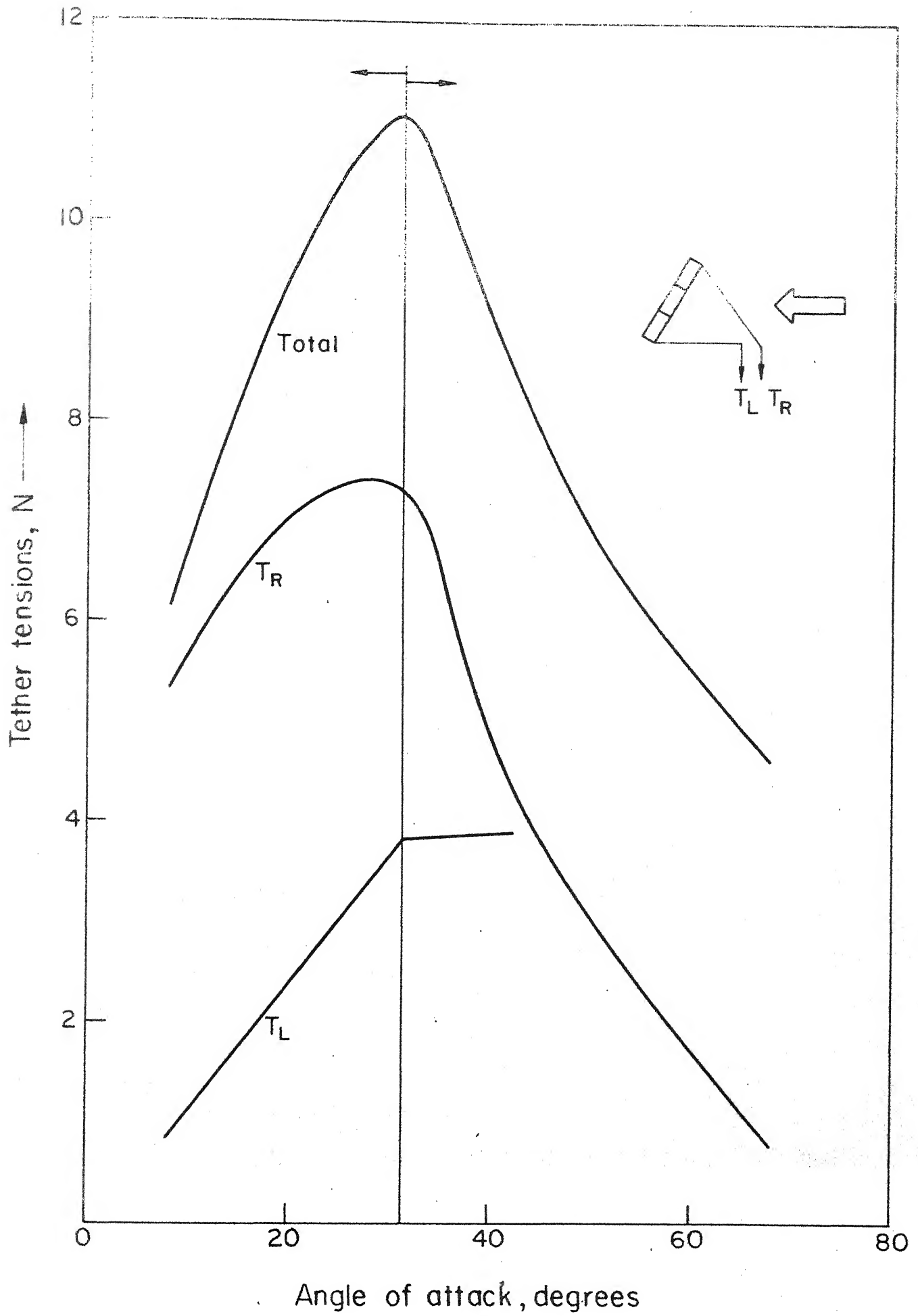


Fig. 12 Variation of kite tether tension with angle of attack  
"Extreme points of fixation"

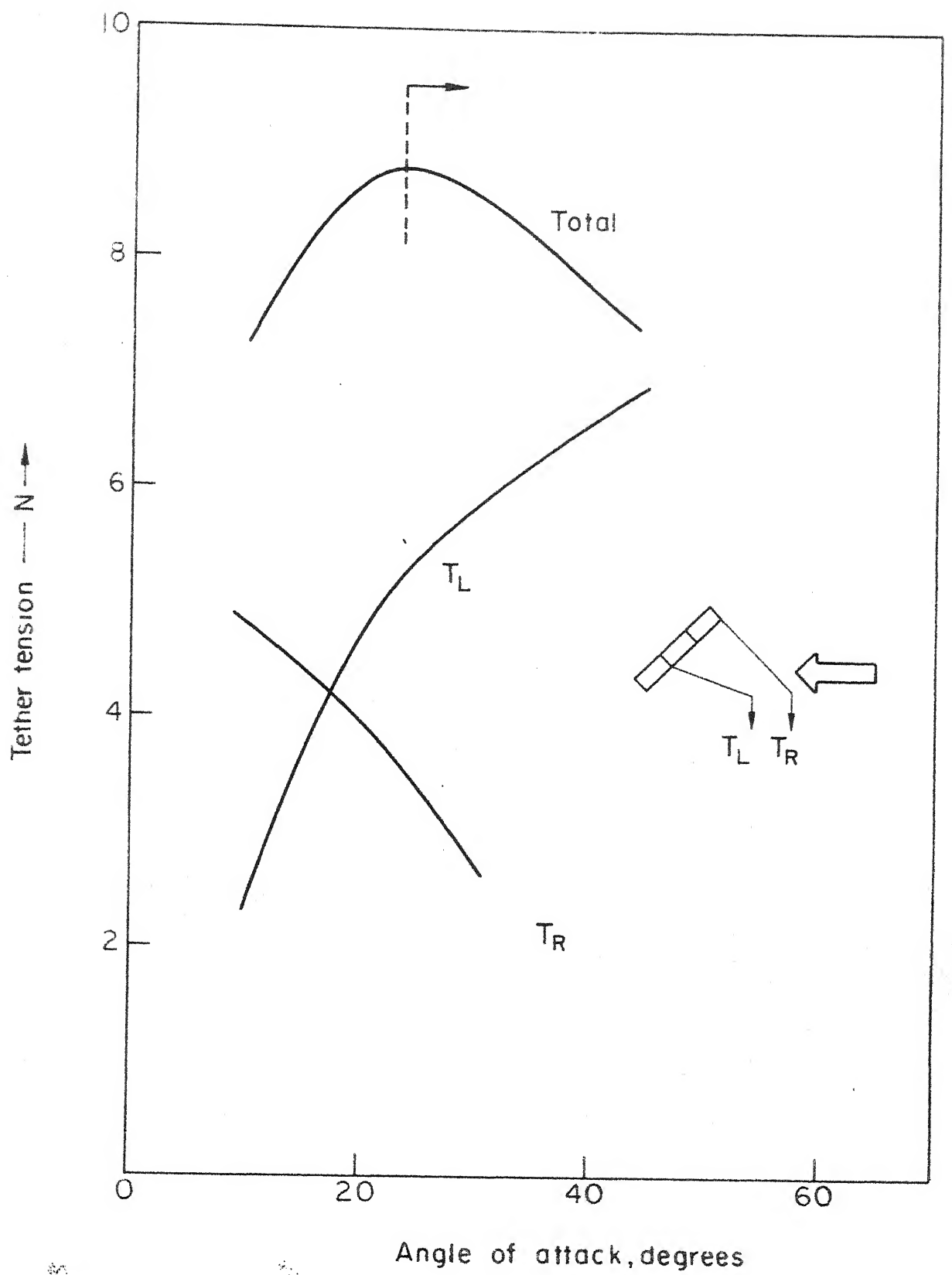


Fig. 13: Variation of kite tether tension with angle of attack "Nearest points of fixation."

In conclusion, we can design a kite pump for total tether tension of 11 N when angle of attack is  $32^\circ$  ( $T_R = 7.26$  N,  $T_L = 3.84$  N) and tether tension of 6.18 N ( $T_R = 5.39$  N,  $T_L = 0.79$  N) when angle of attack is  $8^\circ$ .

## CHAPTER V

### DESIGN OF THE KITE PUMP MECHANISM

In this section we wish to design a suitable mechanism, that will utilize the variation in the tether tension available from the kite to pump water. For the successful functioning of the kite pump, the matching of kite characteristics with the lifting of water load is crucial. Since the tether tension varies with the kite angle of attack, we must get two distinct kite attitudes during the upward and downward strokes in order that the mechanism be self operative. The kite angle of attack can be changed by the relative displacement of its tethers. A complete motion cycle for the kite pump can be divided into four parts. In the first part the kite moves upward. During upward motion the kite attitude should be so adjusted that the maximum load is lifted. The load consists of a dead weight-bucket and a useful load-water contained in the bucket. Now, as the system reaches the end of the upward stroke, somehow two things should happen simultaneously to get the system ready for the downward stroke. First, the kite's angle of attack should be changed so that its load lifting capacity reduces. Secondly, the bucket full of water should discard its water by tilting, but it must maintain sufficient dead weight to move the system downward. Thus, there are two relative thread displacements needed, one to change the kite's angle of attack and another to tilt the bucket. The energy to accomplish these relative displacements may come from the system's inertia

during the end of upward and downward strokes. The driving force during the downward stroke is the net difference between the bucket dead weight and the kite tether tension. The moment the system reaches the bottom distination, the tethers should again be relatively displaced in such a way that the original configuration (that of upward stroke) is regained. This can also be accomplished by the use of inertial energy of the system at the end of downward stroke. In this way the system is ready to move upward again. This cycle repeats itself.

After making a lot of trials with different arrangements and adjustments, the mechanism shown in Fig.14 was found to meet our requirements.

#### V-1 MECHANISM DESCRIPTION (FIG.14):

The mechanism consists of a perfectly balanced beam 1 which is free to rotate about a fulcrum 2. At the right end of the beam, a small aluminum lever 3 is attached. The lever is also free to rotate about its hinge. There is a spring 4 that connects the lever tip with the beam and stores the energy when the whole system changes configuration at two deadpoints. Because of motion requirements, the total rotation of the beam and the lever are restricted to  $60^\circ$  and  $90^\circ$  respectively. Pins 5 and 6 restrict the beam rotation and 7 and 8 do the same for the lever. One kite tether and one bucket string are fixed to the beam end. The other kite tether that changes the kite's angle of attack and the other bucket string which tilts

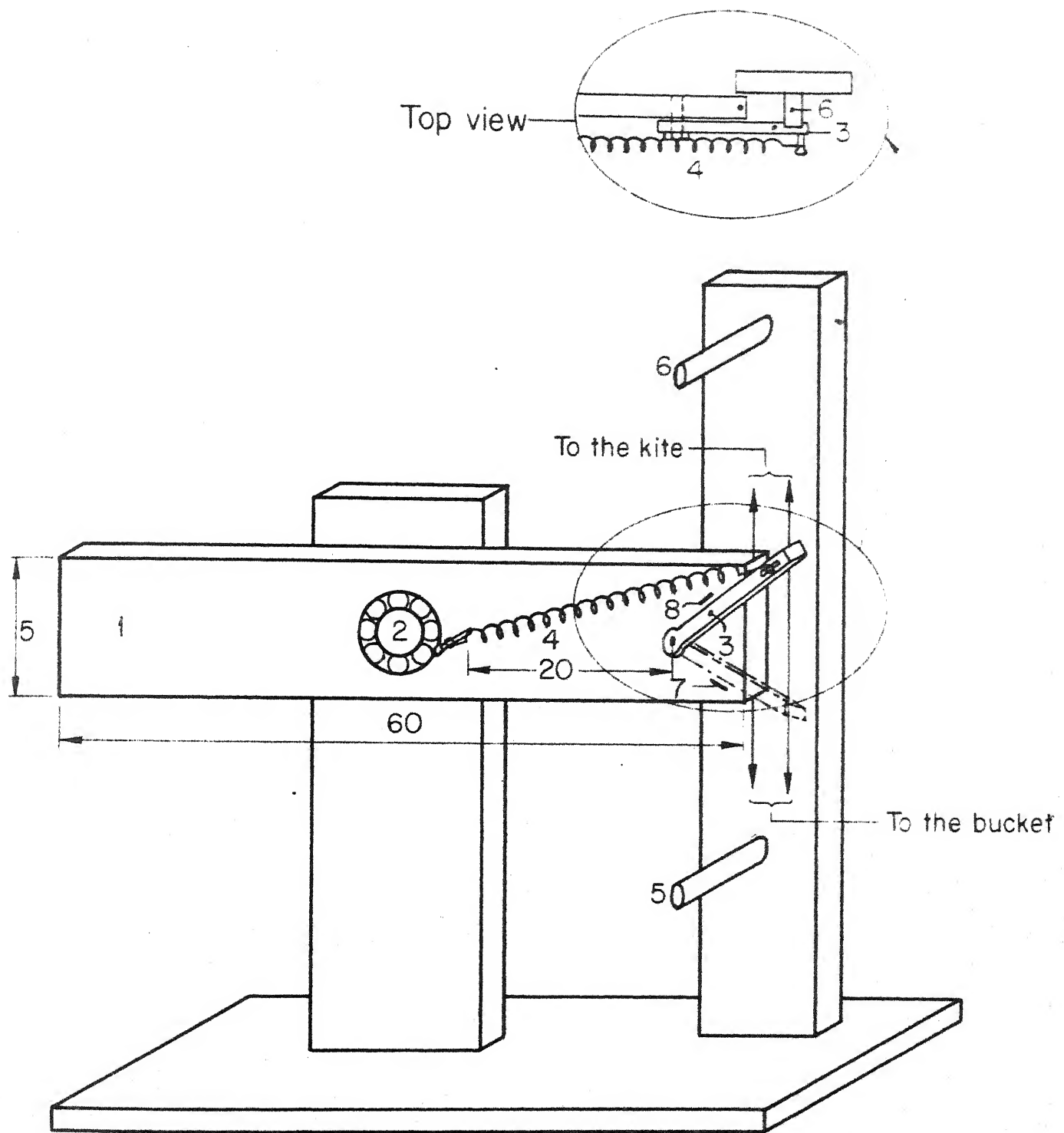


Fig.14 The mechanism of kite pump

the bucket are both fixed to the lever tip.

#### V-2 WORKING OF THE KITE PUMP MECHANISM

At the start of the upward stroke, the kite's attitude is adjusted to obtain the maximum lifting capacity. The bucket is full of water, but the force due to the dead weight + water load is slightly less than total tension in the kite tether. This unbalance force causes an upward movement (accelerates) of the beam end, lever, bucket and the kite system as a whole, without having any relative motion among themselves. When the lever encounters pin 6, its tip portion comes to rest, while the beam end along with the kite and bucket continues to move upward with quickly diminishing velocity. This is shown in Fig.15(a). The angular kinetic energy acquired by the beam during its upward stroke, goes into the expansion of the spring which is connected with the clockwise turning lever. Spring assists in turning the lever very quickly, after the lever passes through the stage when the lever fulcrum and the spring endpoints fall on the same straight line. It is clear here, that the lever acts as a switch, having only two equilibrium positions because of the spring.

The upward beam motion ceases when the lever finishes its clockwise turn. In the meantime kite changes its angle of attack and the bucket discards its water load by tilting. This all happens because of the relative tether displacement provided by the lever movement. Due to all these actions, the kite's lifting capacity is reduced so much so that the dead weight of the

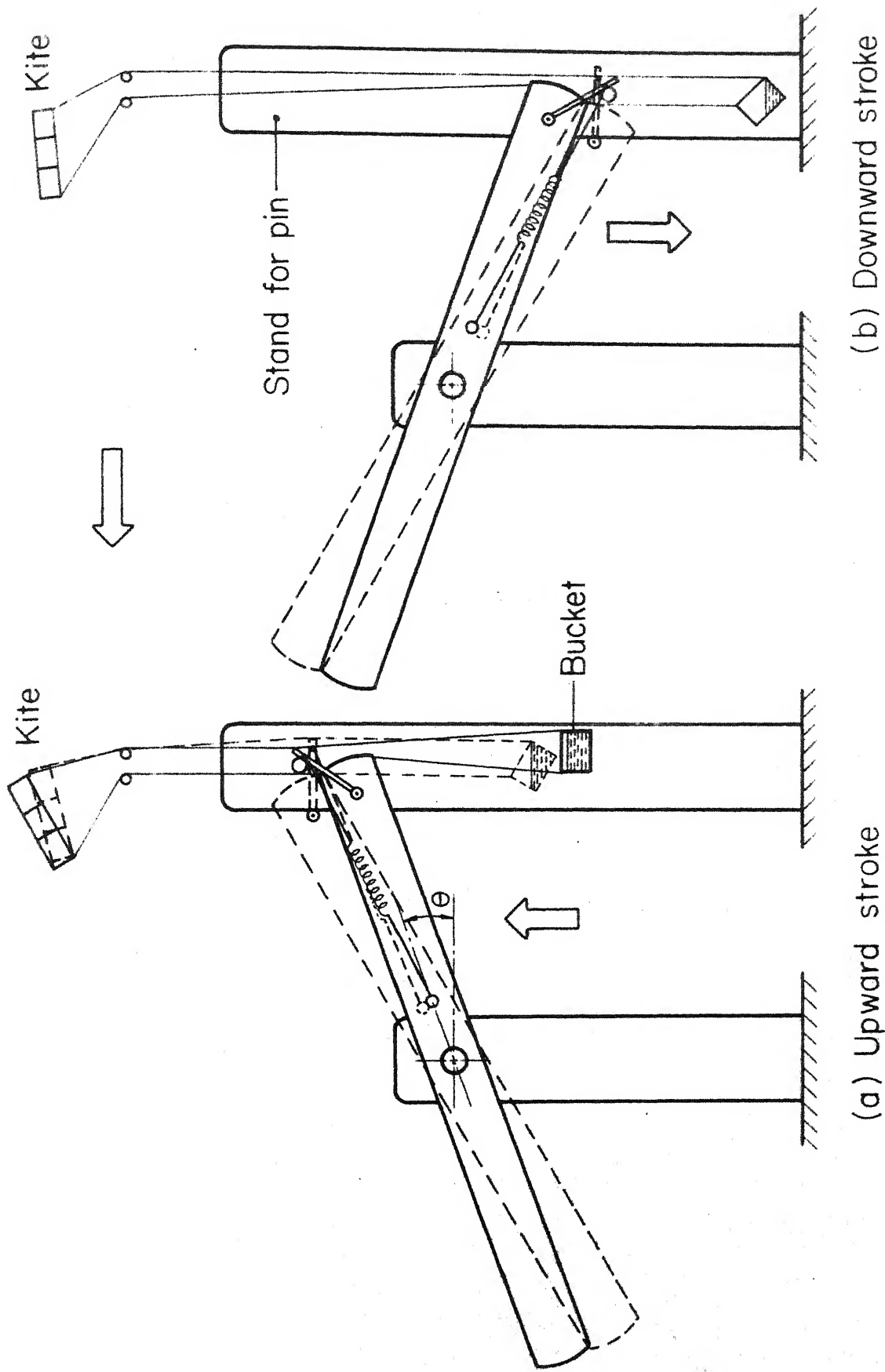


Fig. 15 Working of the kite pump model

bucket is sufficient to start the downward stroke. The beam accelerates and the angular kinetic energy it acquires during its downward stroke is used to turn the lever counterclockwise, when the latter encounters the bottom pin 5. This rotation of the lever causes the kite to regain its original angle of attack; for maximum lifting capacity. It also lifts the bucket to become normal and full of water. This is shown in Fig.15(b). Since the kite's lifting capacity is much more than the sum of bucket's dead weight and the water load, upward motion starts and the cycle is repeated.

### V-3 DETERMINATION OF DESIGN PARAMETERS

Now we specify the design criterions which will lead to an optimum design of the kite pump.

Upward motion: Since the kite is constrained to move vertically in the wind tunnel, the region to the left of the peak of the total tension curve (Fig.12) is selected. From Section IV, we have the kite load pulling capacity as

$$\text{maximum tether tension } (T_{R1} + T_{L1}) = (7.26 + 3.84) = 11.0 \text{N for } 32^\circ \text{ angle of attack}$$

$$\text{minimum tether tension } (T_{R2} + T_{L2}) = (5.39 + 0.79) = 6.18 \text{N for } 8^\circ \text{ angle of attack}$$

The dead weight + weight of water in upward stroke and dead weight in downward stroke are related to the tether tensions by two parameters:

$$\text{Water load parameter } x_1 = \frac{DW + W_{H_2O}}{T_{R1} + T_{L1}} ; \quad x_1 < 1$$

$$\text{Dead weight parameter } x_2 = \frac{DW}{T_{R2} + T_{L2}} ; \quad x_2 > 1$$

During the beam's upward motion, the system acceleration may be calculated by balancing the torque around the fulcrum, as given below for any angular position  $\theta$  with horizontal (Fig.15)

$$\int_0^{L/2} \sigma_b g A x dx - \int_0^{L/2} \sigma_b g A x dx - (DW + W_{H_2O}) \frac{L}{2} \cos \theta \\ + (T_{R1} + T_{L1}) \frac{L}{2} \cos \theta = [ (m_k + \frac{W_{H_2O}}{g}) (\frac{L}{2} \cos \theta)^2 + I ] \alpha_1$$

(1)

where  $x$  is the distance of the element  $A dx$ , along the beam from the beam fulcrum and  $m_k$  is the mass of kite which is 30 gms.

After simplification equation 1 becomes

$$\alpha_1 = \frac{[(T_{R1} + T_{L1}) - (DW + W_{H_2O})](L/2 \cos \theta)}{I + (\frac{W_{H_2O}}{g} + m_k)(\frac{L}{2} \cos \theta)^2} \quad (2)$$

including water load parameter and Dead weight parameter, expression becomes

$$\alpha_1 = \frac{(1 - x_1)[T_{R1} + T_{L1}] \frac{L}{2} \cos \theta}{I + (\frac{x_1(T_{R1} + T_{L1})}{g} + m_k)(\frac{L}{2} \cos \theta)^2} \quad (3)$$

in writing eq. [ 1 ] and [ 2 ] we have made following assumptions:

- ( i ) The beam is perfectly balanced about its fulcrum
- ( ii ) Tether mass is negligible
- ( iii ) Two kite and bucket tethers are connected very close to each other

From eq. [ 3 ] we see that angular acceleration  $\alpha_1$  is a function of  $\theta$ , the angle that the beam makes with horizontal. However, its variation with  $\theta$  is not large and therefore a mean value is used in further calculations. Once  $\alpha_{m1}$  is determined the final angular and linear velocities can be obtained from

$$\nu_{f1} = (2 \times \alpha_{m1} \times \phi)^{1/2} \quad (4)$$

$$V_{f1} = \nu_{f1} \times \frac{L}{2} \quad (5)$$

$$\text{and the time for upward stroke } t_1 = \nu_{f1} / \alpha_{m1} \quad (6)$$

As the system approaches the end of its upward stroke, the lever strikes the pin and its one end stops, the other end keeps on turning along with the beam. As the lever rotates about the pin, two actions occur simultaneously-tilting of the bucket and reduction in the kite's angle of attack. Both these movements will now be analysed in detail.

**Bucket tilting:** The bucket dimensions have been selected to be  $3 \times 4 \times 5 \text{ cm}^3$  to hold 53 gm of water (for  $x_1 = 0.75$  and  $x_2 = 1.25$ ).

The bucket should empty before the lever end reaches its lower extreme position. Fig.16 shows several positions of the tilting bucket and Table 3 shows the tension in the bucket strings. Figure 17 shows that the tension in the bucket's right string i.e.  $T'_R$  reduces faster than the kite tether tensions  $T_R$  and  $T_L$  and it goes to zero when the relative tether displacement reaches 4 cm approximately (the full range is 10 cm). Thus after lever turns completely, the bucket is empty and the dead weight is carried only by the string tied to the beam.

Now the turning of lever requires that the beam should have sufficient angular kinetic energy to do so. The beam at the end of its upward stroke gains an angular kinetic energy of  $\frac{1}{2}I\nu_{f1}^2$ . Assuming that the initial spring extension is very small, that the energy required to change the kite's angle of attack is negligible and 20% of beam angular kinetic energy is lost during impact; we can determine the spring stiffness K by balancing the beam's angular kinetic energy with the spring's potential energy

$$K = \frac{0.80 I \nu_{f1}^2}{x^2} \quad (7)$$

But the constraints on the lever motion are:

(i) The lever should not turn by itself during the downward stroke. From Fig.12 of section IV,  $T_{R2} = 5.3N$  at the minimum kite pulling capacity. Therefore, the spring should be capable of exerting moment greater than  $(5.3 \times 5)N\text{ cm}$  in order to avoid self turning of the lever. One choice freely available is to

TABLE 3BUCKET STRING TENSIONS AS IT DISCARDS THE WATER BY TILTING

For Water load parameter  $x_1 = 0.75$   
 Dead weight Parameter  $x_2 = 1.25$   
 Bucket dimensions  $3 \times 4.6 \times 5$  cm.  
 Dead weight of the bucket = 7.569 N  
 (without water)  
 Water load = 0.525 N

S.No. (Bucket positions)	Relative string displacement, cm	Weight of the water in the bucket, N	$T_L$ , N	$T_R$ , N
1	0	0.677	4.123	4.123
2	2.6	0.338	5.805	2.102
3	4.0	0.155	7.674	0.050

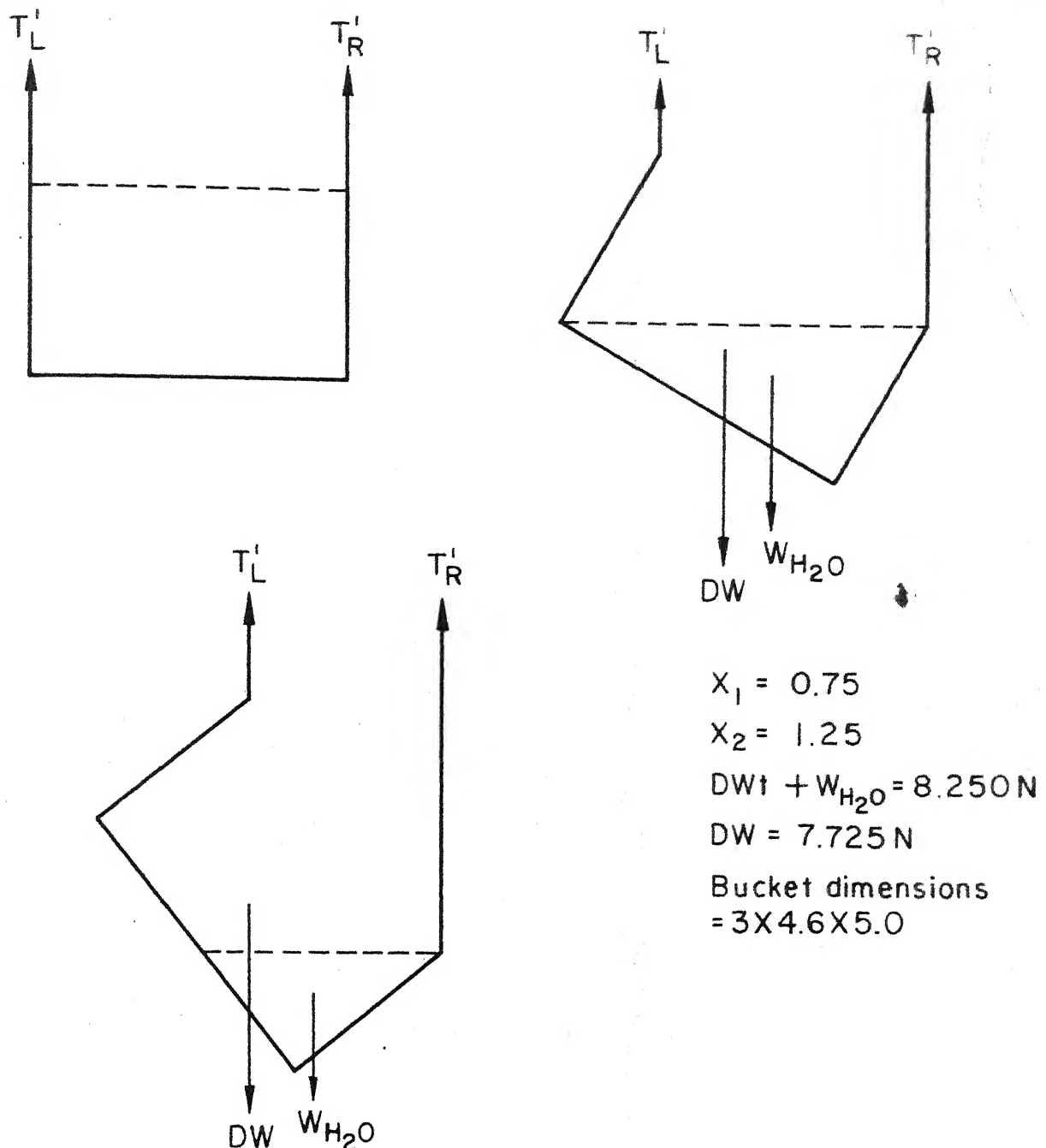


Fig. 16 Representation of the tilting bucket as it discards the water load.

$X_1 = 0.75$   
 $X_2 = 1.25$   
 $DW + W_{H_2O} = 8.250\text{N}$   
 $DW = 7.725\text{ N}$   
 Bucket dimensions =  $3 \times 4.6 \times 5.0\text{ cm}$

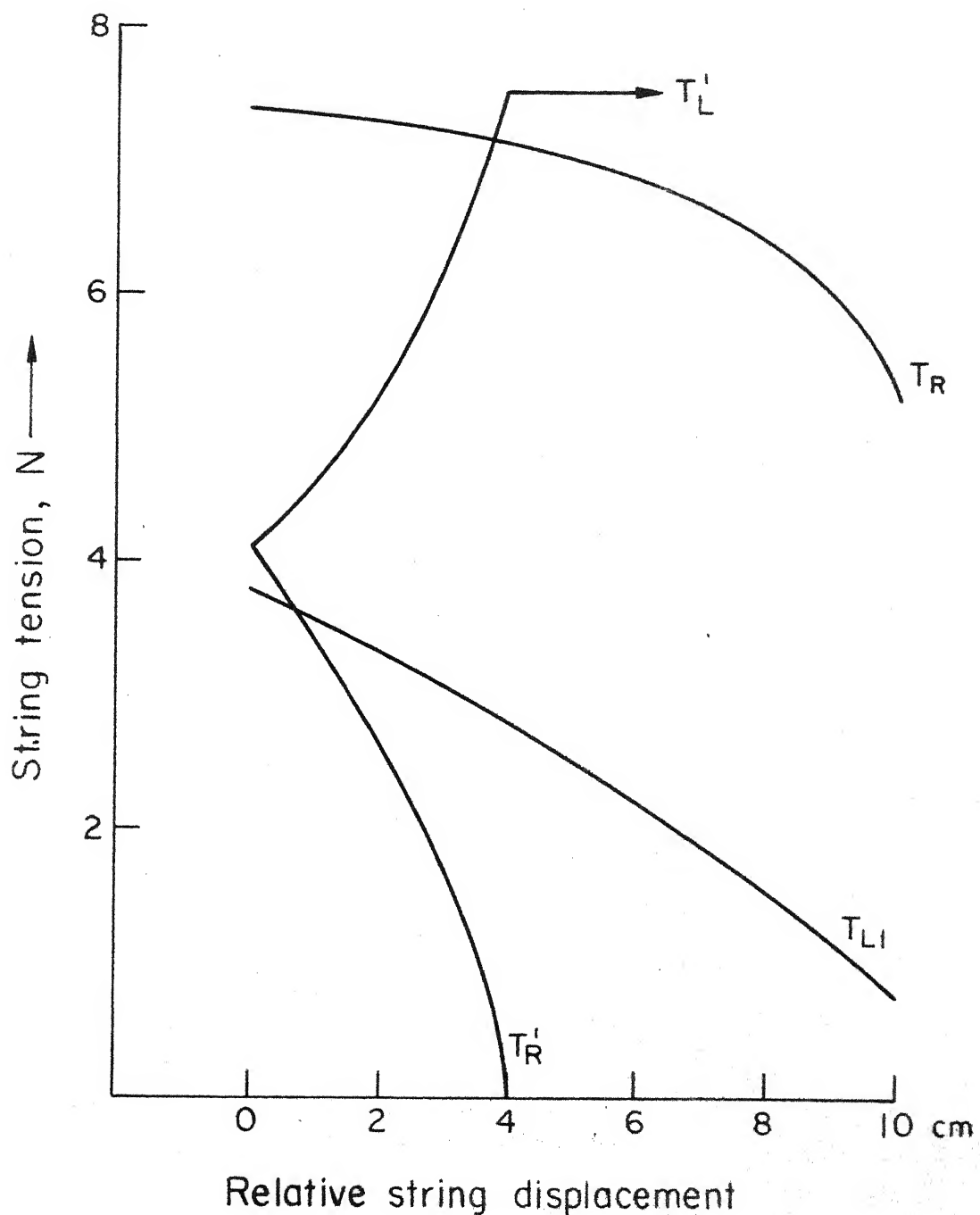
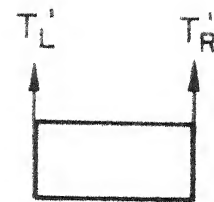


Fig. 17 The string tension variation of a tilting bucket

to increase the moment arm of the spring force. For this, the spring is fixed on the beam at the maximum possible distance of 20 cm from the lever fulcrum. This geometry gives a moment arm of 4.07 cm for the spring force and spring extension of 1.66 cm. These considerations determine the minimum stiffness of spring. However, final values of the spring stiffness can only be determined after the downward motion is complete satisfactorily.

(ii) In the upper lever position i.e. when it is touching the pin 6 (Fig.14), self turning is impossible, because  $T_R > T'_R$  and the spring force is assisting in avoiding self turning.

Now to fix the beam dimensions, we note that it must have sufficient angular kinetic energy so that the lever can turn from the one extreme position to the other against the force of spring. Due to space limitations, the beam length should not exceed 60 cm and the kite's stroke length (which is equal to the distance moved by the beam end) by 30 cm. For the beam to have sufficient angular kinetic energy to turn up the lever when the latter is stopped by the pin, a beam length of more than 100 cm is required if the beam material is taken to be aluminum. Therefore, it cannot be used even though it is inexpensive. Copper is excellent but it is somewhat expensive. Mild steel can be used in place of copper if the beam thickness is slightly increased. From all these considerations, we get for

	Beam length	Width	Thickness
Copper	60 cm	5.0 cm	1.00 cm
Mild steel	60 cm	5.0 cm	1.13 cm.

Moreover, for 30 cm of kite stroke, total angle of beam rotation comes out to be  $60^\circ$ .

About the lever dimensions also, some remarks are in order. To keep the two top and bottom tether fixing points very close, the lever fulcrum is located towards the beam fulcrum. It has been found while conducting experiments that approximately 10 cm of relative tether displacement is needed to change the kite's angle of attack by  $24^\circ$ . To get this relative tether displacements, the length of the lever and its total angular oscillation range has been selected as 7.10 cm and  $90^\circ$  respectively.

Downward motion: For the beam's downward motion, under the same assumptions as we have used for upward motion, the equation of motion is obtained by taking moment about the beam fulcrum-

$$[DW - (T_{R2} + T_{L2})] \frac{L}{2} \cos\theta = [I + (\frac{DW}{g} + m_k)(\frac{L}{2} \cos\theta)^2] \alpha_2 \quad (8)$$

noting that  $W_{H_2O} = 0$  and  $DW = x_2 (T_{R2} + T_{L2})$  this becomes

$$\alpha_2 = \frac{(x_2 - 1)(T_{R2} + T_{L2}) \frac{L}{2} \cos\theta}{I + [x_2 \frac{(T_{R2} + T_{L2})}{g} + m_k](\frac{L}{2} \cos\theta)^2} \quad (9)$$

The mean angular acceleration  $\alpha_{m2}$ , final angular and linear velocity and the stroke time  $t_2$  are determined from

$$\nu_{f2} = (2 \times \alpha_{m2} \times \emptyset)^{1/2} \quad (10)$$

$$V_{f2} = \nu_{f2} \times \frac{L}{2} \quad (11)$$

$$t_2 = \nu_{f2} / \alpha_{m2} \quad (12)$$

Spring stiffness is determined from the energy conservation when the lever strikes the bottom pin and turns counterclockwise.

Again a 20% impact loss is assumed

$$K = \frac{0.80 I v_{f2}^2}{x^2} \quad (13)$$

The iteration between the requirements of upward and downward strokes yield a spring stiffness of 14 N/cm and an initial spring extension of 0.5 cm.

#### V.4 CYCLE PERFORMANCE PARAMETERS

The total water load per cycle can be calculated from

$$m_{H_2O} = \frac{(DW + w_{H_2O}) - DW}{g} \quad (14)$$

or,

$$m_{H_2O} = \frac{x_1 (T_{R1} + T_{L1}) - x_2 (T_{R2} + T_{L2})}{g} \quad (15)$$

The mass flow rate is given by

$$\dot{m}_{H_2O} = \frac{x_1 (T_{R1} + T_{L1}) - x_2 (T_{R2} + T_{L2})}{g (t_1 + t_2)} \quad (16)$$

The power developed by the pump,  $P = \dot{m}_{H_2O} g h$

and the power coefficient is  $PC = P / \frac{1}{2} \sigma_a v^2 s$

where  $S$  is the kite's surface area.

CENTRAL LIBRARY  
I.I.T., Kanpur.

Acc. No. A-82408

82407

### V.5 OPTIMIZATION

Since the water load per cycle, the mass flow rate and power; all depend upon the water load parameter  $X_1$  and the dead weight parameter  $X_2$ ; an optimization with respect to these parameters is necessary. Computer outputs for these calculations are presented in the appendix. Based on these results Figs.18-21 have been drawn. Fig.18 shows the variation of water load per cycle with the dead weight parameter  $X_2$  for different values of the water load parameter  $X_1$ . We see that as  $X_1$  increases and  $X_2$  decreases, the water load per cycle increases as expected. Fig.19 depicts the mass flow rate as a function of  $X_2$  for different values of  $X_1$ . The peak of curve shifts towards right as  $X_1$  increases and a cross over takes place at  $X_1 = 0.90$ . Also, the curves become more steep as  $X_1$  increases i.e. the variation in  $X_2$  affects the mass flow rate to a larger extent as  $X_1$  increases. The optimum value of mass flow rate ( $= 0.136 \text{ Kg/sec}$ ) is obtained when  $X_2 = 1.122$  and  $X_1 = 0.90$ . Power follows the same pattern because it is simply mass flow rate multiplied by a constant ( $gh$ ). Therefore power curves have not been plotted here. For the fixed optimum value of  $X_2$  ( $= 1.122$ ), mass flow rate and water load per cycle are plotted in Fig.20, as function of  $X_1$ . This figure shows that mass flow rate and water load per cycle cannot be maximized simultaneously.

It will be interesting to compare the output power and mass flow rate of this kite pump at optimum design conditions with the existing centrifugal and propellar type pumps used for irrigation purposes. For the same mass flow rate of  $0.136 \text{ Kg/sec}$

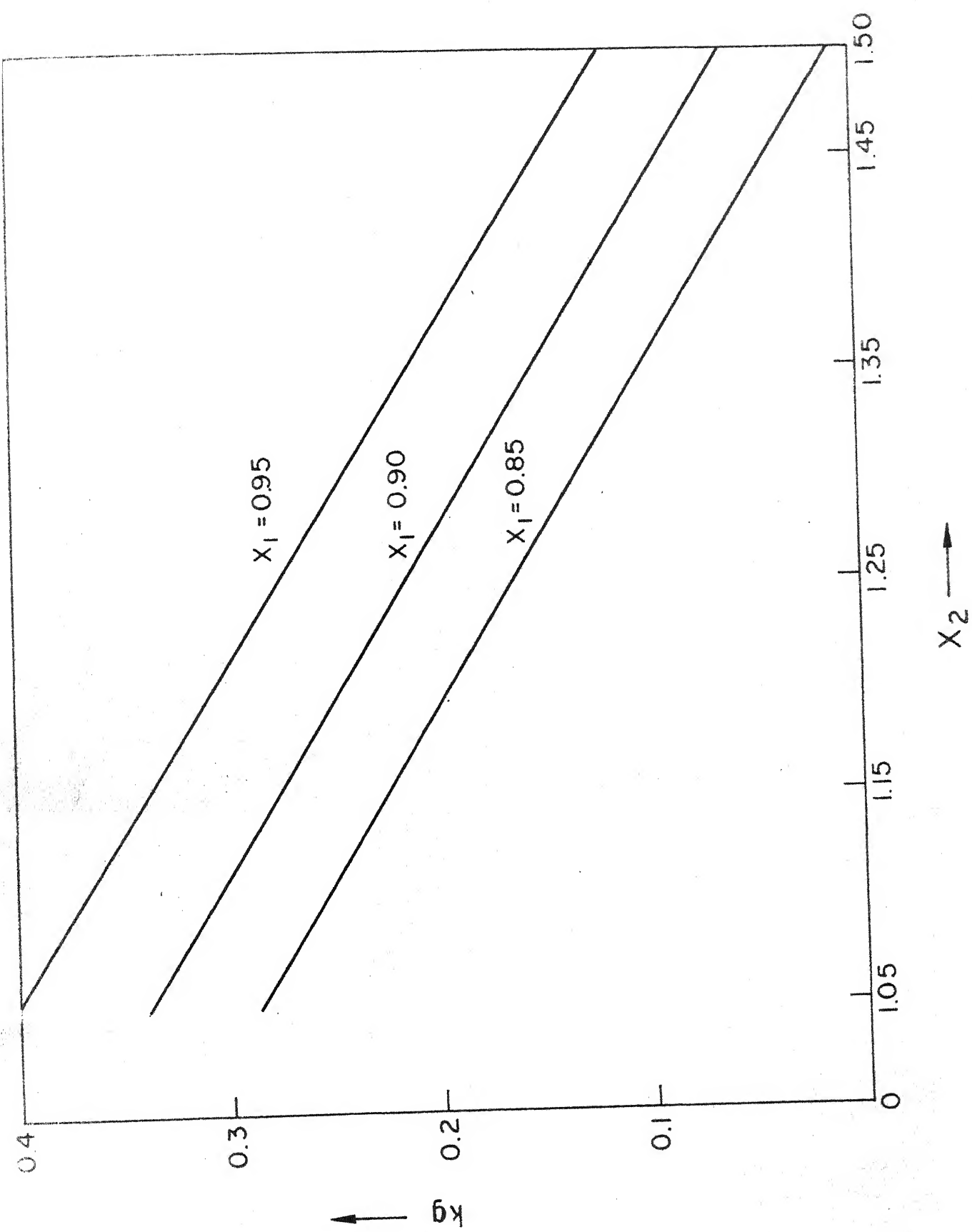


Fig. 18 Dependence of water load on the water load parameter and the dead weight parameter

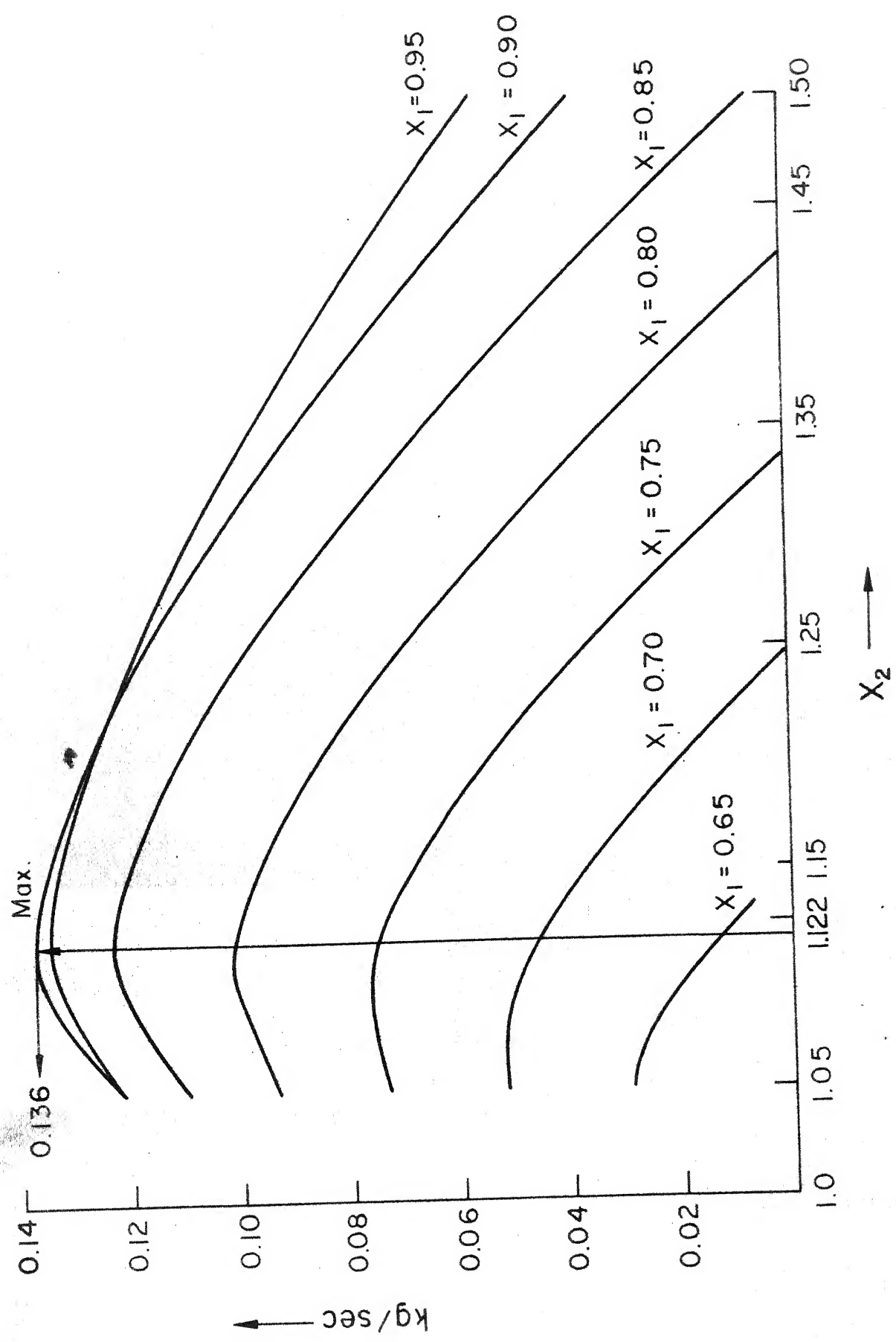


Fig. 19 Variation of mass flow rate with water load parameter and dead weight parameter.

Fig. 19

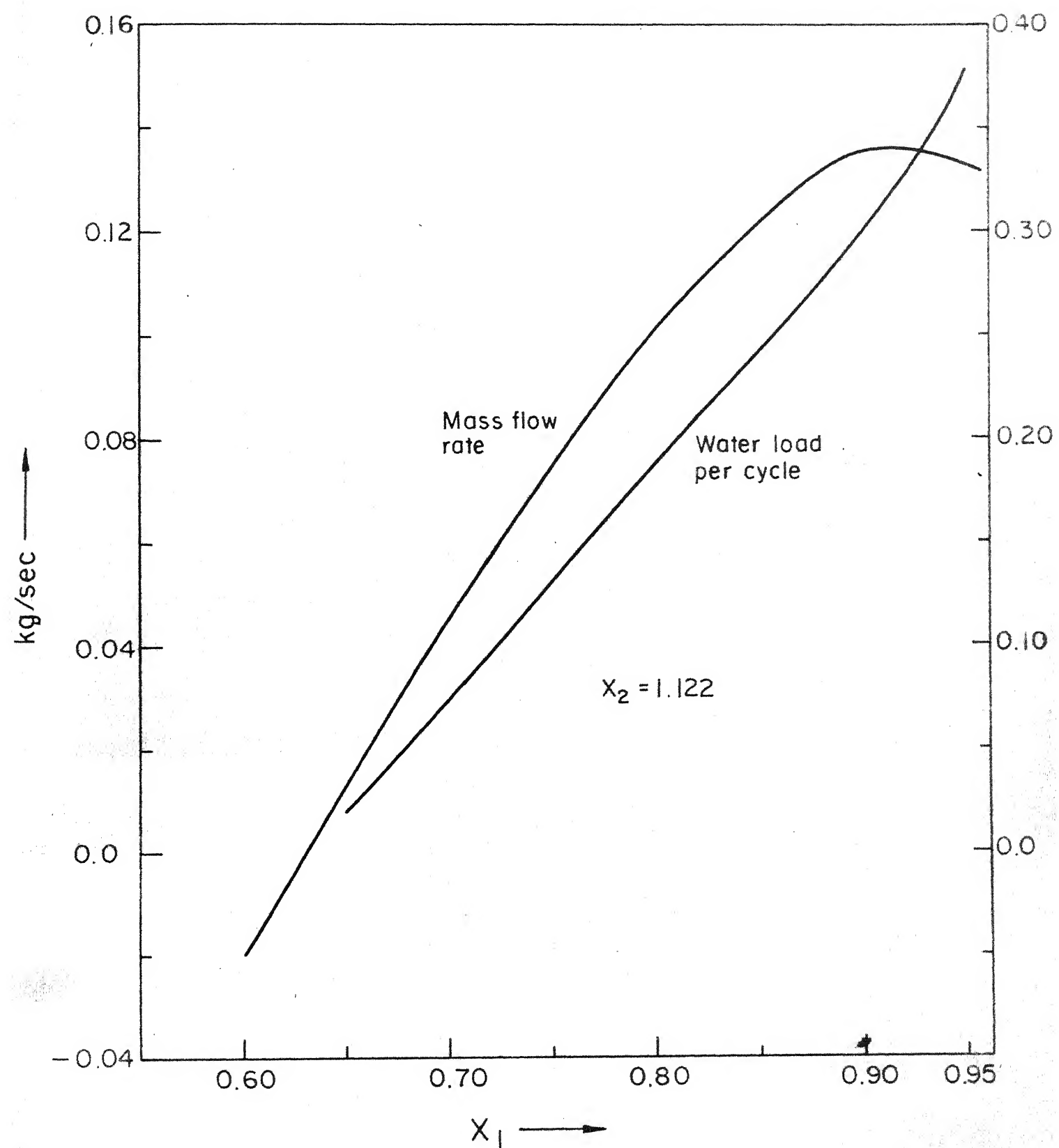


Fig. 20 For a dead weight parameter of 1.122, the variation in water load and mass flow rate with water load parameter.

and 0.40 watts of power added to water, a centrifugal pump with the same inlet and outlet diameters requires merely 0.64 watts (= 0.00086 HP) to be supplied from some external source such as electric motor or diesel engine. The output of kite pump model is comparatively very small, but it is still useful since it takes input energy from a renewable source.

#### V.6 SENSITIVITY ANALYSIS

In an experimental work, it is not unusual to have some variations in the value of parameters recorded. We have determined water load per cycle mass flow rate by varying  $T_{R1}$ ,  $T_{R2}$ ,  $T_{L1}$ ,  $T_{L2}$  each by  $\pm 20\%$ . Computer output is given in appendix and the effect is shown in Fig.21. This figure shows that the water load per cycle and the mass flow rate, are more sensitive to  $T_{R1}$ ,  $T_{R2}$  rather than  $T_{L1}$  and  $T_{L2}$ . Moreover, it is also clear that an increase in  $T_{R1}$  and  $T_{L1}$  is beneficial, whereas the same pattern is detrimental in the case of  $T_{R2}$  and  $T_{L2}$ . This analysis has been done for optimum values of the water load parameter ( $x_1 = 0.90$ ) and dead weight parameter ( $x_2 = 1.122$ ) only.

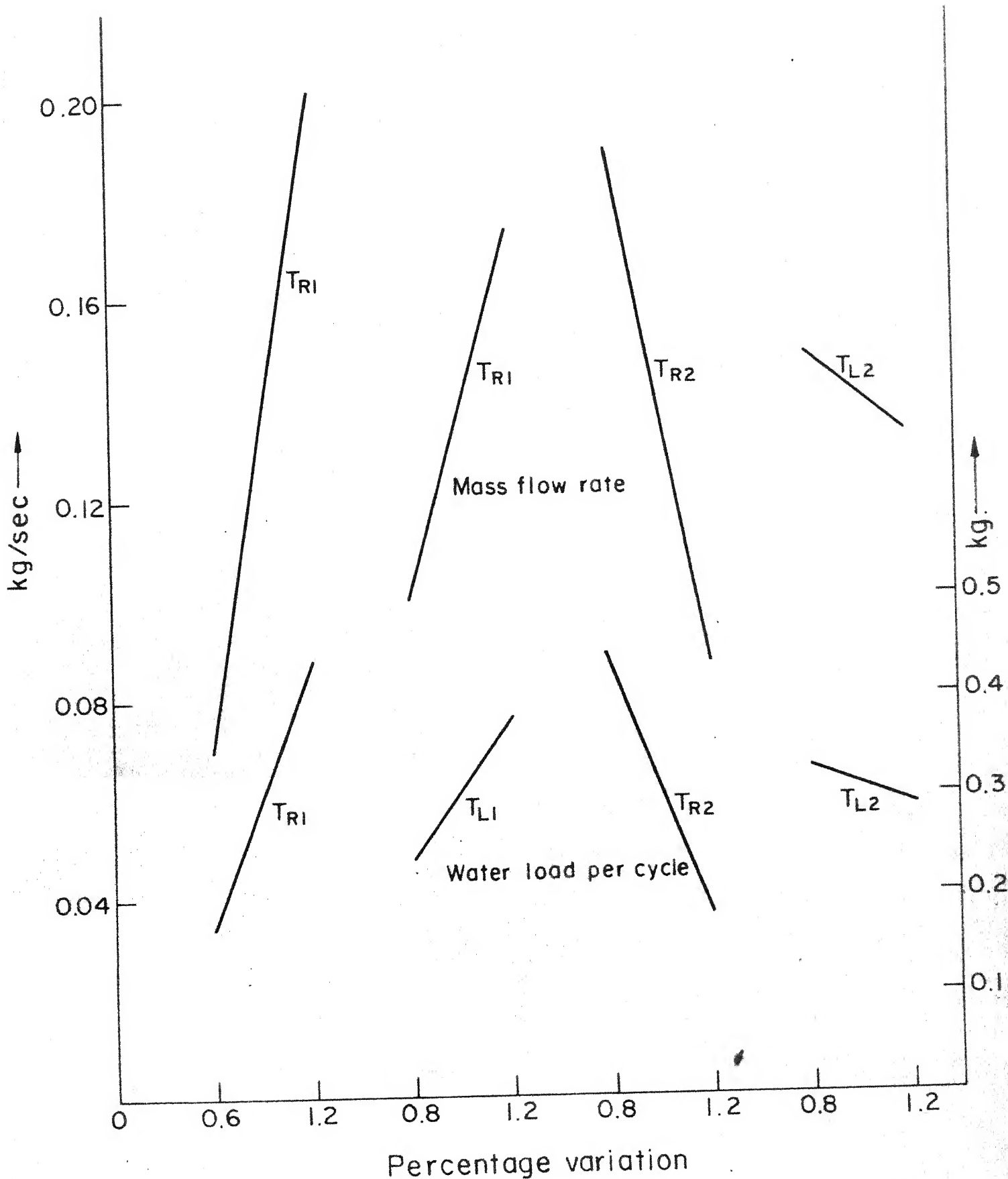


Fig. 21 Dependence of the mass flow rate and the water load per cycle, on the kite tether tension

## CHAPTER VI

### CONCLUSION

A kite pump model for testing in the wind tunnel has been designed. It is a simple, purely mechanical and automatic system in which a bucket is used to lift water. Equations of motion were developed and based on various criterions, design parameters have been selected. Optimization of the water load parameter and dead weight parameter is carried out to obtain maximum mass flow rate and power. The optimum water load and dead weight parameter comes out to be 0.90 and 1.122 respectively. Using a Conyne kite of area  $0.069 \text{ m}^2$  and wind speed of 9 m/sec. The mass flow rate and power turns out to be 0.136 kg/sec and 0.4 watt. This power is equivalent to an input power of 0.64 watt to a centrifugal pump. Further, a sensitivity analysis has been carried out to find out how  $\pm 20\%$  variation in the tethers tension affect the performance parameters of the kite pump. Results indicate that the parameters (e.g. mass flow rate) are more sensitive to the tension of that tether which is connected to the lever rather than the one connected to the beam. Optimum values of the massflow rate and Power, independent of kite area and wind velocity are  $0.219 \text{ kg/sec} \cdot \text{m}^2 \cdot \text{m/sec}$  and  $0.644 \text{ W/m}^3 \cdot \text{sec}$ .

CHAPTER VII  
SUGGESTION FOR FUTURE WORK

This thesis describes the design of a kite pump model. Now it should be fabricated and its functioning should be demonstrated. Based on the experience and outcome of its working, the design should be modified and extended to the design and fabrication of the prototype system. These prototype system can be compared with the existing irrigation pumps and the economic justification of the new system should be sought. There are several important questions that must be answered before the economics can be clearly understood. Whether some new mechanisms for the same purpose can be explored? Whether the same lever mechanism will be able to furnish the relative thread displacements needed in case of large kites flying at high attitudes. List of questions still remains, but this work provides a methodology for more detailed design and prototype study of such wind energy conversion system.

REFERENCES

1. W.Heronemus "WIND POWER" McGraw Hill Encyclopedia of Science and Technology, 14, 647-649 (1982).
2. C.A.J.Fletcher and B.W.Roberts, "Electricity Generation from jet stream winds", Journal of Energy 3, 241-249 (July-Aug. 1979).
3. M.L.Loyd, "Cross Wind Power", Journal of Energy 4, 106-111 (May-June 1980).
4. J.S.Goela, "Project Report-I on Wind Energy Conversion Through Kites" DST Report No.DST/ME(JSG)/81-84/I, Department of Mechanical Engineering, IIT Kanpur (January 1982).
5. Create a Kite published by Simon and Schuster, 124-128 (1977).
6. J.S.Goela and Manoj Jain, "How does a Kite Fly?" Science Today, 16, 44-50 (January 1982).
7. J.L.McKinley and R.D.Bent, Basic Science for Aerospace Vehicles: 4th Ed. McGraw Hill Book Co. (1972).
8. The Kite site advertisement in; Kite lines Journal 2, Number 4, 16-17, (Fall 1979).
9. A. Pope Wind Tunnel Testing, 2nd Ed. John Wiley and Sons, 120-121 (1964).

## APPENDIX

## OPTIMIZATION OF MASS FLOW RATE WITH RESPECT TO WATER LOAD PARAMETER AND DEAD WEIGHT PARAMETER

CONT.

THE REFINED DENOISE-WEIGHT PARAMETERS FOR DETERMINED  
BY EIGENFUNCTION FACTORS IN THE WATER-LEVEL PARAMETERS

$\gamma_2=1.192$

$\alpha$	$w_{11}$	$w_{12}$	$T_1$	$M_{12}$	$D_{12}$	$T_2$	$M_{22}$	$D_{22}$	$\beta$	$v$	$\beta^*$
.90	1.147	1.362	0.479	1.542	1.799	1.166	-1.021	-0.031	-0.061	-0.002	
.95	1.731	1.026	1.521	1.542	1.799	1.166	-0.013	0.022	0.030	0.001	
.70	3.413	3.463	1.572	1.542	1.799	1.166	-0.043	0.073	0.132	0.004	
.75	5.175	3.295	0.637	1.542	1.799	1.166	-0.073	0.134	0.219	0.007	
.80	1.714	2.902	0.723	1.542	1.799	1.166	-0.101	0.192	0.296	0.009	
.85	2.921	2.475	0.847	1.542	1.799	1.166	-0.122	0.246	0.360	0.011	
.90	1.891	1.902	1.053	1.542	1.799	1.166	-0.136	0.302	0.401	0.013	
.95	0.939	1.389	1.510	1.542	1.799	1.166	-0.134	0.353	0.394	0.012	

## SENSITIVITY ANALYSIS

 $x_1=0.90$  $x_2=1.122$ 

X1	X2	X3	X4	ALM1	OMF1	T1	ALM2	OMF2	T2	MDOT	M	P	PC
1.0	1.0	1.0	1.0	2.10	0.998	1.72	1.90	1.1044	0.1778	0.3738	0.5233	0.016	
1.0	1.0	1.0	1.0	2.10	0.998	1.70	1.89	1.1109	0.1858	0.3919	0.5469	0.017	
1.0	1.0	1.0	1.0	2.10	0.998	1.68	1.87	1.1177	0.1938	0.4100	0.5703	0.017	
1.0	1.0	1.0	1.0	2.10	0.998	1.57	1.81	1.1542	0.2310	0.4971	0.6798	0.021	
1.0	1.0	1.0	1.0	2.10	0.998	1.55	1.80	1.1628	0.2385	0.5152	0.7018	0.021	
1.0	1.0	1.0	1.0	2.10	0.998	1.53	1.79	1.1709	0.2458	0.5333	0.7234	0.022	
1.0	1.0	1.0	1.0	2.10	0.998	1.40	1.72	1.2209	0.2796	0.6204	0.8229	0.025	
1.0	1.0	1.0	1.0	2.10	0.998	1.38	1.70	1.2327	0.2863	0.6385	0.8424	0.026	
1.0	1.0	1.0	1.0	2.10	0.998	1.35	1.68	1.2451	0.2927	0.6566	0.8615	0.026	
1.0	1.0	1.0	1.0	2.05	0.997	1.012	1.72	1.900	1.1044	0.1434	0.3034	0.4219	0.013
1.0	1.0	1.0	1.0	2.05	0.997	1.012	1.70	1.89	1.1109	0.1514	0.3214	0.4457	0.014
1.0	1.0	1.0	1.0	2.05	0.997	1.012	1.68	1.87	1.1177	0.1595	0.3395	0.4693	0.014
1.0	1.0	1.0	1.0	2.05	0.997	1.012	1.57	1.81	1.1542	0.1970	0.4267	0.5798	0.018
1.0	1.0	1.0	1.0	2.05	0.997	1.012	1.53	1.79	1.1628	0.2045	0.4447	0.6020	0.019
1.0	1.0	1.0	1.0	2.05	0.997	1.012	1.40	1.72	1.2209	0.2463	0.5500	0.7250	0.022
1.0	1.0	1.0	1.0	2.05	0.997	1.012	1.38	1.70	1.2327	0.2531	0.5680	0.7449	0.023
1.0	1.0	1.0	1.0	2.05	0.997	1.012	1.35	1.68	1.2451	0.2597	0.5861	0.7644	0.023
1.0	1.0	1.0	1.0	2.05	0.997	1.012	1.30	1.60	1.1044	0.1093	0.2329	0.3216	0.010
1.0	1.0	1.0	1.0	2.05	0.997	1.012	1.27	1.50	1.1109	0.1174	0.2510	0.3455	0.010
1.0	1.0	1.0	1.0	2.05	0.997	1.012	1.25	1.48	1.1542	0.1255	0.2691	0.3692	0.011
1.0	1.0	1.0	1.0	2.05	0.997	1.012	1.22	1.40	1.1628	0.1633	0.3562	0.5031	0.015
1.0	1.0	1.0	1.0	2.05	0.997	1.012	1.20	1.38	1.2327	0.1709	0.3743	0.5252	0.016
1.0	1.0	1.0	1.0	2.05	0.997	1.012	1.17	1.35	1.2451	0.1785	0.3923	0.6278	0.019
1.0	1.0	1.0	1.0	2.05	0.997	1.012	1.15	1.30	1.1717	0.1863	0.4795	0.6481	0.020
1.0	1.0	1.0	1.0	2.05	0.997	1.012	1.12	1.28	1.1542	0.1942	0.2270	0.5156	0.020
1.0	1.0	1.0	1.0	2.05	0.997	1.012	1.10	1.25	1.1628	0.2020	0.2406	0.3325	0.010
1.0	1.0	1.0	1.0	2.05	0.997	1.012	1.08	1.22	1.1717	0.2099	0.2587	0.3564	0.011
1.0	1.0	1.0	1.0	2.05	0.997	1.012	1.05	1.18	1.1211	0.2176	0.2768	0.3801	0.011
1.0	1.0	1.0	1.0	2.05	0.997	1.012	1.02	1.15	1.1292	0.2254	0.3639	0.4915	0.015
1.0	1.0	1.0	1.0	2.05	0.997	1.012	1.00	1.12	1.1746	0.2382	0.5138	0.5138	0.016



FANGSØ · A